Finite-Element Modelling of Buoyancy-Driven Flow in Natural Geothermal Systems

Master of Science Thesis in Applied Mathematics

Marie Horn Saltnes

Department of Mathematics
University of Bergen

May 27, 2010

Abstract

Finite element modelling of buoyancy driven flow in geothermal systems is presented in this thesis. The main focus is on the development of a numerical modelling tool. The program developed is tested for classical benchmarks and correspondence with analytical values for the critical Rayleigh-Darcy numbers for onset of convection and Nusselt numbers for various scenarios is shown.

Preface

The program presented in this paper, WAFLE, is a finite element based program for studying buoyancy-driven flow in geothermal systems. WAFLE is based upon the finite element program FANTOM [1] developed by Cedric Thieulot, which is a program for modelling plate tectonics. The program WAFLE was established as a part of this thesis and has been developed in cooperation with Cedric Thieulot.

Outline

This master thesis consists of 7 chapters. The motivation and approach for studying buoyancy-driven flow in natural geothermal systems are presented in Chapter 1. In Chapter 2 the governing equations for fluid flow in porous media are introduced, while Chapter 3 provides the reader with the dimensionless version of the model equations followed by a brief analysis of linear stability.

The finite element method (FEM) is described in Chapter 4, which contains a introduction of the idea and general concepts of standard finite elements, before the FEM applied to transient problems is presented. The numerical modelling tool developed, WAFLE, is presented in Chapter 5. A description of the setup of the program and benchmarks performed are also included. Chapter 6 gives a survey of the preliminary results, and the last chapter summarizes the work done in the development of the numerical modelling tool and proposes recommendations for further work.

Acknowledgement

First of all I would like to thank my supervisors, Inga Berre, Cedric Thieulot and Riske Huismans, for all their help and support. Their enthusiasm and dedication to the project have been indispensable. I would also like thank my fellow students at the Department of Mathematics. Finally, I would like to thank my family and friends.

Contents

Preface **I**

1 Introduction **1**

2 Mass and fluid flow in porous media **3**
2.1 Porosity . . . 3
2.2 Fluid properties . . . 4
2.2.1 Density . . . 4
2.2.2 Viscosity . . . 4
2.3 Permeability . . . 5
2.4 The continuity equation . . . 6
2.5 Model equations . . . 7
2.6 Equation of state . . . 8
2.6.1 The Bousinessq approximation . . . 9

3 Dimensionless model equations and linear stability analysis **11**
3.1 Dimensional analysis . . . 11
3.2 Dimensionless model equations . . . 12
3.2.1 Dimensionless numbers for natural convection . . . 13
3.2.2 Other dimensionless numbers for convectional flow . . . 15
3.3 Linear stability analysis . . . 16

4 Numerical Methods **19**
4.1 The finite element method . . . 20
4.1.1 Variational Formulation . . . 20
4.1.2 The Galerkin Method . . . 22
4.1.3 Extension to general boundary conditions . . . 25
4.1.4 General domains . . . 27
4.2 Finite element methods for transient problems . . . 31
4.2.1 A semidiscrete scheme in space . . . 32
4.2.2 Fully discrete schemes . . . 33
4.3 The SUPG method . . . 37

5 The numerical modelling tool **39**
5.1 WAFLE 39
5.2 Set up and implementation 39
5.2.1 A brief presentation of the set up of WAFLE 39
5.3 Weak formulation 42
5.4 Solver 43
5.4.1 BLAS and LAPACK 44
5.4.2 PARDISO 44
5.5 Benchmarking 45
5.6 Selected types of benchmarks 45
5.6.1 Diffusion benchmark 46
5.6.2 Advection benchmark 50
5.6.3 Heat production 57
5.7 General comments about WAFLE 58

6 Preliminary numerical results **59**
6.1 Measure and computation of Rayleigh numbers and corresponding Nusselt numbers 59
6.1.1 The critical Rayleigh-Darcy number 59
6.1.2 Computation of Rayleigh-Darcy numbers and corresponding Nusselt numbers 60

7 Summary and further work **65**
7.1 Summary 65

Bibliography **67**

Chapter 1

Introduction

Geothermal energy is in general terms the thermal energy stored in the Earth's crust. Thermal energy in the earth is distributed between the constituent host rock and the natural fluids that are contained in its fractures and pores at temperatures above ambient levels. These fluids are primarily water with varying amounts of dissolved salts, and are typically present in their liquid phase. Under certain conditions, they may be in a liquid-vapour mixed phase or in a superheated steam vapour phase.

Logical and regional geologic and tectonic phenomena play a major part in determining the location and quality of a particular geothermal resource, for instance, depth, position, fluid chemistry and temperature. Tectonic plate boundaries and areas of geologically recent igneous activity and/or volcanic events are often associated with regions of high heat flow, and hence, geothermal energy. However, other areas must not be neglected in the consideration of possible opportunities for extraction of geothermal energy.

The heat flow is usually due to two primary processes, upward convection and conduction of heat from the Earth's mantle and core, and heat generated by the decay of radioactive elements in the crust. Due to similarities between extraction of geothermal energy and the extraction of oil, gas and coal, and mining, techniques and terminology have been borrowed or adapted for development of geothermal energy. Hence, the extension of regions where extraction of geothermal energy may be possible is immense.

The energy is extracted from the reservoir by a coupled transport process consisting of convective heat transfer in porous and/or fractured regions of rock and conduction through the rock itself. Typically, hot water or steam is produced and its energy is converted into a marketable product, such as electricity or process heat.

Another interesting phenomena within geothermal systems is the occurrence of buoyancy-driven flow, as the convection effects the temperature distribution in the system.

Processes of transport and other physical processes can be represented in the form of partial differential equations as the equations are expressions of rates of changes, and solving these equations the physical processes can be modelled.

When solving differential equations, the goal is to find a function that satisfies a given relationship between various of its derivatives on some given region of space and/or time, along with boundary conditions along the edges of the domain. This is in general difficult, and an analytical formulation for the solution can only rarely be found.

Numerical methods are often used for solving partial differential equations, and in the case of solving elliptic, parabolic and hyperbolic partial differential equations, the finite difference method (FDM) and the finite element method (FEM) are the most common numerical methods.

Chapter 2

Mass and fluid flow in porous media

In order to better describe the physics governing the studied processes, we introduce hereafter the definitions of the physical quantities describing the types of media under consideration. What follows is mainly based upon the book by Bear [2].

2.1 Porosity

A porous medium consists of solid and void spaces where the void spaces, or pores, are interconnected such that fluid can flow through the medium. The porosity is a dimensionless quantity measured by

$$\phi = \frac{V_P}{V_B},$$

where V_P is the volume of the pore space and V_B is the bulk volume or total volume of the medium.

Within a porous medium, there may be dead-end pores and isolated pores in addition to the interconnected network of pores. A dead-end pore is a pore or channel with only one narrow connection to the interconnected pore space, while an isolated pore has no connection to the interconnected pore space. When studying fluid flow through a porous medium, the dead-end pores and the isolated pores have no influence regarding the observed flow rate. The effective pore space, consisting exclusively of the interconnected pore space, is then introduced. Hence, an expression for the effective porosity ϕ_e, is obtained:

$$\phi_e = \frac{V_{Pe}}{V_B},$$

where V_{Pe} is the effective pore volume.

In this paper, the term porosity will be used when effective porosity is the quantity referred to. Therefore, the notation ϕ will represent effective porosity.

2.2 Fluid properties

2.2.1 Density

Fluid density, denoted by ρ_f, is defined as the mass of the fluid per unit volume. The density of a fluid varies in general with temperature and pressure, and the relation between these properties is called an equation of state:

$$\rho_f = \rho_f(T, p).$$

Density has the SI-unit kg/m^3.

2.2.2 Viscosity

Another property used to characterise fluids is viscosity. Fluids may be defined as materials that continue to deform in the presence of any shearing stress. This continuous deformation is referred to as 'flow', while viscosity is a measure of the ability of the fluid to resist deformation. The viscosity of a fluid varies in general with temperature and pressure. However, for most fluids the viscosity is insensitive to pressure, compared to the temperature dependence, until rather high pressures have been attained. Hence, the viscosity is usually considered as a function of temperature only:

$$\mu = \mu(T),$$

where T is the temperature of the fluid. The viscosity μ are sometimes referred to as the dynamic viscosity. Expressed in SI-units, viscosity has the dimension Pa·s, or kg/ms.

For pure fluids, treating the viscosity as constant is a valid assumption. Since we are only considering flow of water in geothermal systems, the viscosity will be assumed to be constant throughout this thesis.

Laminar flow

A term often touched upon when the viscosity of a fluid is discussed, is laminar flow. Laminar flow is fluid flow in which the fluid travels smoothly or in regular paths. This phenomenon occurs when the velocity, pressure and other fluid properties remain constant at each point in the fluid. Laminar flow is only common for certain situations. Typical settings would be narrow channels, slow moving fluid and relatively high viscosity. Flow of oil through a thin tube or blood flowing through capillaries are examples of laminar flow.

Turbulent flow

For turbulent flow, magnitude and direction of the speed of the fluid at a point are changing continuously, which result in swirls and eddies as the bulk of the fluid is moving in one specific direction. Some common examples of turbulent flow

are oceanic and atmospheric currents, blood flow in arteries and oil transport in pipelines.

The dimensionless Reynolds number,

$$Re = \frac{\rho V L}{\mu},$$

is an important quantity when characterising the behaviour of the flow, whether it is laminar or turbulent. The density is denoted by ρ, V is mean fluid velocity, L characteristic linear dimension (for instance travelled length of fluid) and μ is the dynamic viscosity of the fluid. The Reynolds number will be futher discussed in Chapter 3 when dimensional analysis is treated.

The Reynolds number is in general less than 2300 for laminar flow and greater than 4000 for turbulent flow. However, the Reynolds number is in this matter dependent of the geometry of the medium the fluid is flowing through. Thus, these values of transition may vary.

Transitional flow

In the transition zone between laminar and turbulent flow, the flow is characterised as transitional flow. It is a mixing of laminar and turbulent flow with turbulent flow in the centre and laminar flow near the edges.

2.3 Permeability

In 1856, the French engineer Henry Darcy investigated the flow of water in vertical homogeneous sand filters. He did a series of experiments with water flowing through different types of sand in a container of height L and cross-sectional area A, where he measured the rate of flow through the sample. From this, Darcy concluded that the relationship between the rate of flow Q and the sample, could be expressed by

$$Q = \frac{\tilde{K} A \, \Delta p}{L}, \tag{2.1}$$

where $\Delta p = p_1 - p_2$ is the difference in pressure between the top and the bottom of the sample, and $\tilde{K}$ is a coefficient of proportionality depending on the rock. Darcy's law is only valid for laminar flow at small velocities.

The coefficient of proportionality, or hydraulic conductivity, $\tilde{K}$, can be expressed in terms of viscosity and density, (see [2] for further details):

$$\tilde{K} = \frac{K \rho g}{\mu},$$

where K is the permeability and g is the gravity. The permeability depends on the properties of the porous medium, such as the grain or poresize distribution, and is

a measure of the ability of the medium to transmit fluids. The unit of permeability is Darcy. Converted to SI-units, 1 Darcy $\approx 0.987 \cdot 10^{-12}\text{m}^2$.

Sandstone and limestone are typical oil and gas reservoir rocks with a permeability of $10^{-1} - 10^4$ mD (milli-Darcy). Rocks with permeabilities of $10^2 - 10^8$ mD, like sand and gravel, are highly permeable. An example of a low permeable rock is granite, which has a permeability of 10^{-5} mD.

In general, the permeability of a medium is dependent on spatial location and direction of flow. When the properties of the medium varies with the spatial location, the permeability depends on the position

$$K = K(x, y, z),$$

and the medium is said to be heterogeneous. In the opposite case, when K is constant, the medium is homogeneous. Including the dependence of direction of flow, it is convenient to express the permeability as a tensor, $\mathbf{K}$. When the permeability depends on the direction of flow, the medium is anisotropic. A medium independent of direction of flow is isotropic.

After Darcy carried out his original experiment, it has been repeated under more general conditions using different types of fluids and letting the fluid flow in different directions. The generalised form of Darcy's law is

$$\mathbf{v} = -\frac{\mathbf{K}}{\mu}\left(\frac{\Delta p}{L} + \rho g \cos\theta\right), \tag{2.2}$$

where θ is the angle between the direction of flow and the vertical line. When applying (2.2) on a representative elementary volume, Darcy's law on differential form is obtained,

$$\mathbf{v} = -\frac{\mathbf{K}}{\mu}\left(\nabla p + \rho \mathbf{g}\right). \tag{2.3}$$

2.4 The continuity equation

A model of a dynamic system often includes a description of the conservation of a physical quantity, i.e. an extensive variable, when the system is closed. An extensive variable is a physical quantity that is proportional to the mass of the system. For instance, mass and momentum are quantities whose values in a composite system are equal to the sum of their values in each system; hence, they are extensive variables. Intensive variables, on the other hand, are physical quantities that do not depend on the system size or the amount of material in the system. Examples of intensive variables are density, temperature, specific heat and pressure. These quantities are not additive when subsystems are joined.

The conservation equation for an extensive variable is derived by considering the processes that increase or decrease the extensive variable of interest. This is done by developing a balance equation for the extensive quantity contained in a control volume. As the goal is to obtain knowledge about the rate of change of

the quantity evaluated, the conservation equation obtained will have dimension of quantity conserved per time.

Let Ψ be an extensive variable and Ω the domain for our system. The change in Ψ is due to fluxes, $\mathbf{f}$, over the boundary, Γ, and to possible sources and sinks. Mathematically, this can be formulated by the integral equation

$$\int_{\Omega} \frac{\partial \Psi}{\partial t}\, d\Omega + \int_{\Gamma} \mathbf{f} \cdot \mathbf{n}\, d\Gamma = \int_{\Omega} q\, d\Omega, \tag{2.4}$$

where $\mathbf{n}$ is the unit normal vector and q denotes sources and sinks. Applying the divergence theorem gives

$$\int_{\Omega} (\frac{\partial \Psi}{\partial t} + \nabla \cdot \mathbf{f})\, d\Omega = \int_{\Omega} q\, d\Omega. \tag{2.5}$$

The conservation equation is valid for arbitrary domains Ω. This, in addition to continuity of the integrand, leads to the continuity equation on differential form,

$$\frac{\partial \Psi}{\partial t} + \nabla \cdot \mathbf{f} = q. \tag{2.6}$$

In order to obtain the equation of mass conservation for single phase flow, the extensive variable in interest is the mass density m, given by $m = \phi\rho$; the flux density $\mathbf{f}$ is given by $\mathbf{f} = \rho\mathbf{v}$. Hence, the continuity equation for single phase flow is

$$\frac{\partial}{\partial t}(\phi\rho) + \nabla \cdot (\rho\mathbf{v}) = q. \tag{2.7}$$

Note that $\mathbf{v}$ is the Darcy velocity. As opposed to the actual particle flow, the Darcy velocity is a macroscopic measure defined as the flow rate per unit cross sectional area of the porous medium.

2.5 Model equations

In this thesis we consider a single phase flow problem in porous media described by the following equations for energy and momentum.

Energy equations

The energy equations we use for modelling buoyancy driven flow are based on the first law of thermodynamics in a porous medium and are the ones used by Nield and Bejan in *Convection in Porous Media* [3]. We have two energy equations, one for the solid and one for the fluid as we are assuming the temperature of the solid may be different from the temperature of the fluid:

$$(1-\phi)(\rho c)_s \frac{\partial T_s}{\partial t} = (1-\phi)\nabla \cdot (k_s \nabla T_s) + (1-\phi)q_s + h(T_f - T_s), \tag{2.8}$$

$$\phi(\rho c_p)_f \frac{\partial T_f}{\partial t} + (\rho c_p)_f \mathbf{v} \cdot \nabla T_f = \phi \nabla \cdot (k_f \nabla T_f) + \phi q_f + h(T_s - T_f). \tag{2.9}$$

The subscripts s and f denote solid and fluid properties respectively. In these equations, ϕ is the porosity, ρ the mass density, c the heat capacity, k is the thermal conductivity, q the heat production,and h is the heat transfer coefficient between the solid and the fluid. For fluid, a specific heat capacity valid under constant pressure, denoted by c_p, is used. The fluid velocity is denoted by $\mathbf{v}$. As we are modelling fluid flow in porous media, $\mathbf{v}$ is the Darcy velocity expressed by Equation (2.3).

These coupled equations model the temperature change in time in a geothermal system, where the last term on the right hand side in both energy equations allows for heat transfer between the solid and the fluid. As $-k_s \nabla T_s$ is the conductive heat flux through the solid, the term $\nabla \cdot (k_s \nabla T_s)$ represents the net rate of heat conduction into a unit volume of the solid. The factor $(1 - \phi)$ is the ratio of the volume occupied by the solid to the total volume of the medium. Hence, all terms in Equation (3.2) except for the last term on the right hand side, accounting for the heat transfer between the solid and the fluid, are multiplied by $(1 - \phi)$ (as this equation is for the solid only).

Equation (3.3) contains an extra term on the left hand side compared to the energy equation for the solid. This term is due to the Darcy velocity, where $\mathbf{v} \cdot \nabla T_f$ is the rate of change of temperature in the elemental volume due to convection of the fluid into it. Multiplied by $(\rho c_p)_f$, this must be the rate of change of thermal energy per unit volume of fluid, due to the convection.

Under the assumption of local temperature equilibrium, that $T_s = T_f = T$, the two coupled energy equations can be added and reduced to a single equation:

$$(\rho c)_m \frac{\partial T}{\partial t} + (\rho c_p)_f \mathbf{v} \cdot \nabla T = \nabla \cdot (k_m \nabla T) + q_m, \tag{2.10}$$

where

$$\begin{aligned} (\rho c)_m &= (1 - \phi)(\rho c)_s + \phi(\rho c_p)_f, \\ k_m &= (1 - \phi)k_s + \phi k_f, \\ q_m &= (1 - \phi)q_s + \phi q_f, \end{aligned} \tag{2.11}$$

are, respectively, the overall heat capacity per unit volume, overall thermal conductivity, and overall heat production per unit volume of the medium.

2.6 Equation of state

The model equations were introduced in the previous section. Our problem then consists of three equations (2.3, 3.2, 3.3) and four unknown variables: T_s, T_f, $\mathbf{v}$ and p. Hence, an equation of state is needed in order to obtain a closed system of equations.

The presented work focuses on thermal convection. For thermal convection to occur, the density must be a function of temperature. A simple equation of state, as used in [3] amongst others, is given by

$$\rho_f = \rho_0[1 - \beta(T - T_0)], \tag{2.12}$$

where ρ_0 is the density of the fluid at a reference temperature T_0, and β is the thermal expansion of the fluid. Having density as a function of temperature makes the subsequent analysis more intricate. Therefore, we will use the Boussinesq approximation for simplification.

2.6.1 The Bousinessq approximation

Despite the fact that density variations are the essence of buoyancy driven flow, the density is treated as a constant everywhere except in the gravity term when the Boussinesq approximation is applied. That is, density changes are only taken into account in the momentum equation where ρ is multiplied by gravity, $\mathbf{g}$. This leads to the reduced expression for the continuity equation,

$$\nabla \cdot \mathbf{v} = 0. \tag{2.13}$$

This expression for the continuity equation is also obtained when considering incompressible fluids.

For the Bousinessq approximation to be valid, the density changes have to remain small compared to ρ_0 throughout the flow region. In addition to small density changes, the variations in temperature must also be insufficient to cause the various properties of both the fluid and the solid from varying significantly from their mean values.

Chapter 3

Dimensionless model equations and linear stability analysis

Scaling, or nondimensionalisation, and dimensional analysis are two closely related procedures which are often carried out in order to solve a problem. Dimensional analysis ensures that the dimensions of the equations evaluated are correct and is applied for understanding the properties of physical quantities independent of the units used to measure them. Nondimensionalisation, on the other hand, is described by J.D. Murray in [4] as follows: "*Before analysing [a] model it is essential, or rather obligatory to express it in* nondimensional *terms. This has several advantages. For example, the units used in the analysis are then unimportant and the adjectives small and large have a definite relative meaning. It also always reduce the number of relevant parameters to dimensionless groupings which determines the dynamics*".

3.1 Dimensional analysis

According to Fourier's principle of homogeneity, all terms added together in an equation must be of the same dimension. Dimensional analysis is based upon this principle and in this section a procedure for making equations dimensionless will be presented.

Dimensional analysis is a method for reducing complex physical problems by reducing the number of variables that must be specified to describe an event. If equations and/or boundary conditions are not known to their full extent, dimensional analysis may be the only option for solving the problem. The application of dimensional analysis can give quick insight to the problems evaluated, and coupled with its ease of use it often accounts for a large simplification of the equations discussed.

3.2 Dimensionless model equations

In this section the dimensionless equivalent of the model equations will be presented. The dimensionless variables used for obtaining the dimensionless equations are based upon the book by Nield and Bejan, *Convection in Porous Media* [3].

The following equations have been presented in Chapter 2 and are the ones we will make dimensionless:

1. Momentum equation

$$\mathbf{v} = -\frac{\mathbf{K}}{\mu}\left(\nabla p + \rho \mathbf{g}\right). \tag{3.1}$$

2. Energy equations

$$(1-\phi)(\rho c)_s \frac{\partial T_s}{\partial t} = (1-\phi)\nabla \cdot (k_s \nabla T_s) + (1-\phi) q_s + h(T_f - T_s), \tag{3.2}$$

$$\phi(\rho c_P)_f + (\rho c_P)_f \mathbf{v} \cdot \nabla T_f = \phi \nabla \cdot (k_f \nabla T_f) + \phi q_f + h(T_s - T_f). \tag{3.3}$$

3. Continuity equation for nearly incompressible fluids when the Boussinesq approximation is valid

$$\nabla \cdot \mathbf{v} = 0. \tag{3.4}$$

4. Equation of state for density in the case of thermal convection

$$\rho_f = \rho_0[1 - \beta(T - T_0)]. \tag{3.5}$$

As the physical variables contained in the model equations can be expressed in terms of mass, length, time and temperature, four independent coefficients are needed in order to scale the equations and make the size/magnitude of the variables appropriate for modelling. Let M be the characteristic mass, L characteristic length, T characteristic time and θ characteristic temperature. The intention is to express the physical variables in terms of the characteristic quantities and at the same time make them dimensionless. Since we are interested in natural convection, it is desirable to obtain dimensionless coefficients in the model equations that reflect the processes of buoyancy driven flow. By the following choice of dimensionless variables

$$\begin{aligned} &\hat{x} = \frac{x}{L}, \qquad \hat{v} = \frac{vL}{\alpha_f}, \qquad \hat{t} = \frac{t\alpha_f}{L^2}, \qquad \hat{T} = \frac{1-\beta(T-T_0)}{\beta \Delta T}, \\ &\hat{p}_f = \frac{Kp_f}{\mu \alpha_f}, \qquad \hat{q}_f = \frac{q_f L^2}{(\rho c_P)_f \alpha_f \Delta T}, \qquad \hat{h} = \frac{hL^2}{(\rho c_P)_f \alpha_f}, \end{aligned} \tag{3.6}$$

with the kinematic viscosity ν, and the thermal diffusivity α, defined as

$$\nu = \frac{\mu}{\rho}, \qquad \alpha_f = \frac{k_f}{(\rho c_P)_f}, \tag{3.7}$$

the model equations are restated as follows:

1. The dimensionless momentum equation

$$\hat{\mathbf{v}} = -\nabla\hat{p} - RaDa\hat{T}\mathbf{k}. \tag{3.8}$$

2. The dimensionless energy equations

$$\frac{\partial\hat{T}_s}{\partial\hat{t}} = \gamma\nabla^2\hat{T}_s + \gamma\hat{q}_s + \sigma\hat{h}(\hat{T}_s - \hat{T}_f - \frac{T_{s0} - T_{f0}}{\Delta T}), \tag{3.9}$$

$$\frac{\partial\hat{T}_f}{\partial\hat{t}} + \psi\hat{\mathbf{v}}\cdot\nabla\hat{T}_f = \nabla^2\hat{T}_f + \hat{q}_f + \psi\hat{h}(\hat{T}_f - \hat{T}_s - \frac{T_{f0} - T_{s0}}{\Delta T}). \tag{3.10}$$

3. The continuity equation

$$\nabla\cdot\hat{\mathbf{v}} = 0. \tag{3.11}$$

4. The equation of state

$$\hat{\rho_f} = \hat{\rho_0}[1 + \beta\Delta T(\hat{T} - \hat{T}_0)]. \tag{3.12}$$

In the above dimensionless equations, $RaDa$ is the Rayleigh-Darcy number given by

$$RaDa = \frac{\rho_0 g\beta\Delta TKL}{\mu\alpha_f}, \tag{3.13}$$

and

$$\gamma = \frac{\alpha_s}{\alpha_f}, \qquad \psi = \frac{1}{\phi}, \qquad \sigma = \frac{(\rho c_p)_f}{(1-\phi)(\rho c)_s},$$

which are all dimensionless quantities.

3.2.1 Dimensionless numbers for natural convection

Rayleigh number

In the above equations, the dimensionless quantity $RaDa$ appeared. This is the dimensionless Rayleigh-Darcy number, a product of two dimensionless numbers, the Rayleigh number and the Darcy number.

The Rayleigh number for a fluid is associated with buoyancy driven flow, also known as natural or free convection. When the Rayleigh number for the fluid is below a critical value, the heat is transferred primarily through conduction, while for higher Rayleigh numbers, the heat is transferred mainly through convection. Hence, the critical Rayleigh number, Ra_c, determines the onset of convection. For values of Ra lower than Ra_c, no natural convection occurs.

The Grashof number Gr and the Prandtl number Pr are often used for defining the Rayleigh number. It is defined as the product of those two quantities, where

the Grashof number describes the relationship between the buoyancy and the viscosity, while the Prandtl number describes the relationship between the momentum diffusivity and the thermal diffusivity;

$$Gr = \frac{g\beta\ \Delta T\ L^3}{\nu^2}, \qquad \text{and} \qquad Pr = \frac{\nu}{\alpha} = \frac{\mu c_p}{k},$$

where β is the thermal expansion coefficient (also contained in the EOS for density (3.5)), ν is the kinematic viscosity, μ the dynamic viscosity and α is the thermal diffusivity. Hence, the Rayleigh number is the ratio of buoyancy forces and momentum and thermal diffusivity:

$$Ra = GrPr. \tag{3.14}$$

In natural convection, fluid motion is induced by density differences resulting from temperature gradients in the fluid. The Rayleigh number gives an indication of the type of fluid motion as laminar flow typically has Rayleigh numbers between 10^3 and 10^9. For Rayleigh numbers above 10^{12}, the flow is usually turbulent.

When porous media are discussed, the Rayleigh-Darcy number, $RaDa$, is preferred over the Rayleigh number for characterising the fluid motion as permeability is taken into account by the Darcy number,

$$Da = \frac{K}{L^2}, \tag{3.15}$$

where K is the permeability. Thus, the Rayleigh-Darcy number is as presented in Equation (3.13),

$$RaDa = \frac{\rho g\beta\ \Delta T\ LK}{\mu\alpha}, \tag{3.16}$$

where the indices are omitted for simplicity.

Geothermal systems can be modelled as porous media, hence the Rayleigh-Darcy number is the dimensionless number of interest.

Nusselt number

The final dimensionless number treated in this section, is the Nusselt number. This number is the ratio of convective to conductive heat transfer across a boundary within a fluid. The Nusselt number is defined as

$$Nu_L = \frac{hL}{k_f} = \frac{\text{Convective heat transfer}}{\text{Conductive heat transfer}}, \tag{3.17}$$

where h is the (convective) heat transfer coefficient, k_f is the thermal conductivity of the fluid and L is the characteristic length.

A Nusselt number close to unity is often connected to laminar flow, as this value is obtained when convection and conduction are of similar magnitude. Higher Nusselt numbers indicate more active convection and typically Nusselt numbers in the range 100-1000 are related to turbulent flow.

3.2.2 Other dimensionless numbers for convectional flow

In the previous section, dimensionless numbers for natural or free convection in porous media were introduced. These numbers appeared in our equations due to the chosen scaling. When other processes, for instance forced convection, is studied, a different scaling must be carried out and different dimensionless numbers will appear in the equations. For forced convection, the following dimensionless numbers will be of interest.

Reynolds number

The Reynolds number expresses the ratio between the inertial forces and the viscous forces. At very low Reynolds numbers, the viscous forces are the dominating forces, and inertial forces have little effect. On the other hand, at high Reynolds numbers, the viscous forces are negligible while the inertial forces becomes the dominating forces. The Reynolds number is defined as

$$Re = \frac{\rho V L}{\mu}, \tag{3.18}$$

where ρ is the density of the fluid, V the mean fluid velocity, L the characteristic length and μ is the viscosity of the fluid.

The Reynolds number can be used for characterising the motion of the fluid. At low Reynolds numbers, the flow is laminar, while turbulent flow occurs for high Reynolds numbers. There is no sharp interface between the flow being laminar and turbulent flow as the transition is gradual. The transition phase depends on the geometry, but usually the transition zone contains fluid flow with Reynolds numbers from 2300 to 4400. However, for all Reynolds numbers above $10,000$, the flow is turbulent.

Peclet number

The Peclet number is the ratio of the rate of advection of a physical quantity by the flow to the rate of diffusion to the same quantity driven by an appropriate gradient. In the matter of heat transfer, the Peclet number is the product of Reynolds number and the Prandtl number,

$$Pe = RePr = \frac{LV}{\alpha}. \tag{3.19}$$

Archimedes number

The Archimedes number is defined as

$$Ar = \frac{Gr}{Re^2} = \frac{gL^3\rho_f(\rho - \rho_f)}{\mu^2}, \tag{3.20}$$

where ρ_f is the density of the fluid and ρ is the density of the body. This dimensionless quantity is used to determine the motion of the fluid due to density differences

as Ar is the ratio of buoyancy and inertial forces. When analysing mixed convection of a fluid, Ar is used to characterise the dominant type of convection, whether it is natural or forced. When $Ar >> 1$, natural convection dominates, and when $Ar << 1$, forced convection is the dominating convection.

3.3 Linear stability analysis

The linear stability analysis performed in this section is mainly based on the presentation done by Nield and Bejan in *Convection in Porous Media* [3].

For simplicity, we assume the temperature of the solid and the fluid in the model equations above, Equations (3.2)-(3.3), are equal, $T_s = T_f = T$; that the permeability is invariant of time and space; and that the thermal conductivity is constant. The equations we will consider in this analysis are then, cf. Equations (3.4),(3.1),(2.10) and (3.5),

$$\nabla \cdot \mathbf{v} = 0, \tag{3.21}$$

$$\mathbf{v} = -\frac{K}{\mu}\left(\nabla p \ + \rho \mathbf{g}\right) \tag{3.22}$$

$$(\rho c)_m \frac{\partial T}{\partial t} + (\rho c_p)_f \mathbf{v} \cdot \nabla T = k_m \nabla^2 T, \tag{3.23}$$

$$\rho_f = \rho_0[1 - \beta(T - T_0)]. \tag{3.24}$$

The model equations at hand, have a basic steady state solution which satisfies the boundary conditions $T = T_0 + \Delta T$ at the bottom of the domain, $z = 0$, and $T = T_0$ at the top of the domain, $z = L$, see [3]:

$$\mathbf{v}_b = 0, \tag{3.25}$$

$$T_b = T_0 + \Delta T(1 - \frac{z}{L}), \tag{3.26}$$

$$p_b = p - \rho_0 g\big[z + \frac{1}{2}\beta \Delta T(\frac{z^2}{L} - 2z)\big], \tag{3.27}$$

This solution describes the state where heat transfer is only due to conduction.

We now examine the stability of the solution by adding a small perturbation to the solution; the perturbation quantities are denoted with primes. Thus,

$$\mathbf{v} = \mathbf{v}_b + \mathbf{v}', \quad T = T_b + T', \quad p = p_b + p',$$

and substituting these into Equations (3.25)-(3.27), give the following linearised equations when second-order small quantities are neglected:

$$\nabla \cdot \mathbf{v}' = 0, \tag{3.28}$$

$$\mathbf{v}' = -\frac{K}{\mu}(\nabla p' - \beta \rho_0 T' \mathbf{g}), \tag{3.29}$$

$$(\rho c)_m \frac{\partial T'}{\partial t} - (\rho c_p)_f \frac{\Delta T'}{L} w' = k_m \nabla^2 T', \tag{3.30}$$

where $\mathbf{v}' = (u', v', w')$.

Dimensional analysis is then performed on the linearised equations in order to express them on dimensionless form:

$$\nabla \cdot \hat{\mathbf{v}} = 0, \tag{3.31}$$

$$\hat{\mathbf{v}} = -\nabla \hat{p} - RaDa\hat{T}\mathbf{k}, \tag{3.32}$$

$$\frac{\partial \hat{T}}{\partial \hat{t}} - \hat{w} = \nabla^2 \hat{T}, \tag{3.33}$$

where $\mathbf{k}$ is the unit vector in the z-direction. These dimensionless equations arise when L is chosen as the length scale, $\sigma L^2/\alpha_m$ as the time scale, α_m/L as the velocity scale, ΔT as the temperature scale and $\mu\alpha_m/K$ as the pressure scale. The parameters α_m and σ are, respectively, the thermal diffusivity and the heat capacity ratio,

$$\alpha_m = \frac{k_m}{\rho c_p{}_f} = \frac{k_m}{k_f}\alpha_f, \quad \sigma = \frac{(\rho c)_m}{(\rho c_p)_f}.$$

The nondimensional variables obtained are then expressed by

$$\hat{\mathbf{x}} = \frac{\mathbf{x}}{L}, \quad \hat{t} = \frac{\alpha_m t}{\sigma L^2}, \quad \hat{\mathbf{v}} = \frac{L}{\alpha_m}, \quad \hat{T} = \frac{T}{\Delta T}, \quad \hat{p} = \frac{Kp'}{\mu\alpha_m}. \tag{3.34}$$

Taking the curl twice on Equation (3.32) and using (3.31), this expression is obtained when only the vertical component is of interest:

$$\nabla^2 \hat{w} = RaDa\nabla_L^2 \hat{T}, \tag{3.35}$$

where $\nabla_L^2 = \partial/\partial x^2 + \partial/\partial y^2$. We then have two resulting equations, (3.33) and (3.35); two linear equations of two variables. Hence, the equations can be solved by separation of variables [5].

The next step in the analysis, is to substitute the expression for the solution of the problem obtained by separation of variables into Equations (3.33),(3.35), which results in ordinary differential equations. These ordinary equations must be solved due to appropriate boundary conditions; see, for example, Nield and Bejan [3]. The analysis results in the following expression for the Rayleigh-Darcy number,

$$RaDa = \frac{(j^2\pi^2 + \lambda^2)^2}{\lambda^2}, \qquad j = 1, 2, 3, \ldots, \tag{3.36}$$

where λ is the wave number. When $j = 1$, and $\lambda = \pi$, a minimum for the Rayleigh-Darcy number appear. In other words, the critical Rayleigh-Darcy number is

$$RaDa_c = 4\pi^2 = 39.48. \tag{3.37}$$

Hence, for $RaDa_c < 4\pi^2$, the conduction state remains stable and no convection occurs. For $RaDa_c > 4\pi^2$, instability emerges in form of convection cells with horizontal wave number λ.

Chapter 4

Numerical Methods

Due to their complexity, many mathematical problems are not analytically solvable, i.e. the equations cannot be solved conveniently in their original form. For analytical solutions, one often has to make assumptions corresponding to restrictive or special cases, leading to simplified models. As a consequence, concepts, facts and point of views for the reduced problem can be obtained. This can be of high value when working towards the solution to the original, complex problem.

However, the analytical approach is not suitable for a large range of problems and a different one is needed. Solving the problem by using a large number of numerical calculations, i.e. using a numerical method, an approximate solution to the original problem is obtained.

The development of a numerical method consists of combining a small number of general and relatively simple ideas with other knowledge about the type of problem in consideration in an inventive way. Such information is obtainable by, for instance, mathematical analysis and background information of the problem.

Numerical methods are often used for solving partial differential equations. The main idea is to discretise the equations at hand and find a solution to the discrete version of the problem. The problem under consideration has infinitely many degrees of freedom, while the discrete problem has a finite number of degrees of freedom and hence can be solved numerically. To which extent the discrete solution obtained approximates the solution to the equations considered, depends on the numerical method. Several numerical methods exist, and the most suitable method for a given problem is determined by the type of equation in consideration. For solving elliptic, parabolic and hyperbolic partial differential equations, the finite difference method (FDM) and the finite element method (FEM) are the most common numerical methods.

We use the finite element method for solving the problem expressed by the model equations in Chapter 2, and the first part of the chapter consists of a general presentation of the basics of the finite element method. Finite elements for transient (parabolic) problems will be treated in Section 4.2. As will be noted, transient advection-dominated problems arise difficulties when solved with standard finite

elements. In the last section, a method developed to overcome these problems, the SUPG method, will be briefly presented.

4.1 The finite element method

The finite element method approach for discretising the equations starts by rewriting the original problem on differential form and stating it as a variational formulation. Then the variational formulation is discretised by construction of the finite element space V_h and the finite element method for the problem evaluated can be found.

As described in [6], the finite element method is outstanding with respect to handling complicated geometry, general boundary conditions and variable nonlinear material properties. Since the FEM has a clear structure and is versatile, it is possible to construct general purpose software for applications. Furthermore, the theory behind the FEM is comprehensive and hence the method is considered as reliable for solving problems numerically. Another feature of the FEM, is that the error in the solution of the finite element approximation can in many cases be mathematically estimated and analysed.

We say that the FEM is a triple $(K, P(K), \sum_K)$, where K is a geometric object, for instance in 2 dimensions, a triangle or a rectangle; $P(K)$ is a finite dimensional linear space of functions on K; and $\sum_K$ is a set of degrees of freedom such that a function $v \in P(K)$ is uniquely defined by $\sum_K$. These concepts will be treated in the following sections in this chapter. For further details on the FEM than touched upon in this paper, see the books by Braess [7], Johnson [8] and Hughes [9].

4.1.1 Variational Formulation

In this subsection we will first consider a general elliptic differential equation in 2 dimensions. The weak formulations for the problem discussed in this thesis will be derived in Chapter 5. Let

$$\begin{aligned} -\Delta u &= f \qquad \text{in } \Omega, \\ u &= 0 \qquad \text{on } \Gamma, \end{aligned} \tag{4.1}$$

be the problem in consideration. This is a stationary problem where Ω is a bounded domain in the plane with boundary Γ, and f is a given real-valued piecewise continuous function bounded in Ω.

In order to establish the variational formulation or weak form of (4.1), we have to define the linear space

$$\begin{aligned} V = \Big\{ & v : \ v \text{ is a continuous funtion on } \Omega, \\ & \frac{\partial v}{\partial x_1} \text{ and } \frac{\partial v}{\partial x_2} \text{ are piecewise continuous and bounded on } \Omega, \\ & v = 0 \text{ on } \Gamma \Big\}. \end{aligned}$$

Gauss' theorem, often referred to as the divergence theorem,

$$\int_{\Omega} \nabla \cdot \mathbf{F} \; d\Omega = \int_{\Gamma} \mathbf{F} \cdot \mathbf{n} \; d\Gamma, \tag{4.2}$$

where $\mathbf{n}$ is the outward unit normal to Γ, will be needed in the derivation of the variational formulation.

Multiplying (4.1) by a test function $v \in V$ and integrating over the domain Ω gives

$$-\int_{\Omega} \Delta u \; v \; d\Omega = \int_{\Omega} f v \; d\Omega. \tag{4.3}$$

From the product rule for the divergence of the test function multiplied with the gradient of u, we obtain an expression for the left hand side in (4.3),

$$\int_{\Omega} \Delta u \; v \; d\Omega = -\int_{\Omega} \nabla u \cdot \nabla v \; d\Omega + \int_{\Omega} \nabla \cdot (v \nabla u) \; d\Omega. \tag{4.4}$$

Applying Gauss' theorem (4.2) on the second term on the right hand side of (4.4) gives

$$\int_{\Omega} \nabla \cdot (v \nabla u) \; d\Omega = \int_{\Gamma} (v \nabla u) \cdot \mathbf{n} \; d\Gamma, \tag{4.5}$$

which is a boundary integral over the test function. According to our definition of the space V, this integral is zero. Inserting the result from the product rule (4.4) in (4.3), we get a weak form of the original problem (4.1),

$$\int_{\Omega} \nabla u \cdot \nabla v \; d\Omega = \int_{\Omega} f v \; d\Omega \qquad \forall \; v \in V. \tag{4.6}$$

The notations

$$a(u, v) = \int_{\Omega} \nabla u \cdot \nabla v \; d\Omega, \qquad\qquad (f, v) = \int_{\Gamma} f v \; d\Omega$$

are introduced to establish the variational formulation. The form $a(\cdot, \cdot)$ is a bilinear form on $V \times V$, meaning that for $\alpha, \beta \in \mathbb{R}$ and $u, v, w \in V$ we have

$$\begin{aligned} a(u, \alpha v + \beta w) &= \alpha a(u, v) + \beta a(u, w), \\ a(\alpha u + \beta v, w) &= \alpha a(u, w) + \beta a(v, w). \end{aligned}$$

Using this notation, we derive the variational form from the weak form (4.6)

$$\text{Find } u \in V \text{ such that } a(u, v) = (f, v) \qquad \forall \; v \in V. \tag{4.7}$$

4.1.2 The Galerkin Method

The variational formulation obtained in the preceding section provides a good basis for developing the finite element method. In order to discretise the variational formulation, we need to divide our domain Ω into several nonoverlapping partitions. In two dimensions, these partitions can either be triangles or rectangles. If a partition consists of triangles, this partition is called a triangulation. We will consider triangulation when discussing the general theory of the FEM, while a partition of rectangles will be used when setting up the finite element method for the model equations evaluated in Chapter 5.

Partitioning

(i) Triangles

Assume $\Omega \in \mathbb{R}^2$ is a polygonal domain in space. Let T_h be a triangulation of Ω, partitioning the domain into n triangles K, $T_h = \{K\}$. We then define the space $P_r(K)$,

$$P_r(K) = \{v \ : \ v \text{ is a polynomial of degree at most } r \text{ on } K\}, \qquad r = 0, 1, 2, \ldots.$$

For $r = 1$, the space $P_1(K)$ consists of linear functions,

$$v(\mathbf{x}) = v_{00} + v_{10}x_1 + v_{01}x_2,$$

where $\mathbf{x} = (x_1, x_2) \in K$ and $v_{ij} \in \mathbb{R}$, $i, j = 0, 1$. The dimension of $P_1(K)$, $\dim(P_1(K)) = 3$.

For $r = 2$, the space $P_2(K)$ is the proper space for the polynomials, and consists of quadratic functions. Hence,

$$v(\mathbf{x}) = v_{00} + v_{10}x_1 + v_{01}x_2 + v_{20}x_1^2 + v_{11}x_1x_2 + v_{02}x_2^2, \qquad v \in P_2(K),$$

where $v_{ij} \in \mathbb{R}$, $i, j = 0, 1, 2$ and $\dim(P_2(K)) = 6$.

In general, for general $r \in \mathbb{N}$, we have

$$P_r(K) = \{v \ : \ v(\mathbf{x}) = \sum_{0 \le i+j \le r} v_{ij}x_1^i x_2^j, \ \mathbf{x} \in K, \ v_{ij} \in \mathbb{R}\}, \ r \ge 0,$$
$$\dim(P_r(K)) = \frac{(r+1)(r+2)}{2}.$$

(ii) Rectangles

Let Ω be a regular domain, and let K_h be the partition of Ω into nonoverlapping rectangles K such that horizontal and vertical edges of the rectangles are parallel to the x_1- and x_2-coordinate axes respectively. In addition, no vertex of any rectangle

can lie in the interior of an edge of another rectangle. The space of polynomials is then

$$Q_r(K) = \{v : v(\mathbf{x}) = \sum_{i,j=0}^{r} v_{ij} x_1^i x_2^j,\ \mathbf{x} \in K,\ v_{ij} \in \mathbf{R}\},\ r \geq 0,$$
$$\dim(Q_r(K)) = (r+1)^2.$$

In the case where $r = 1$, the corresponding finite element space is

$$V_h = \{v : v \text{ is continuous on } \Omega \text{ and } v|_K \in Q_1(K),\ K \in K_h\}.$$

Hence, the function $v \in Q_1(K)$ is bilinear,

$$v(\mathbf{x}) = v_{00} + v_{10}x_1 + v_{01}x_2 + v_{11}x_1x_2,$$

and $\mathbf{x} = (x_1, x_2) \in K$, $v_{ij} \in \mathbb{R}$. As in the triangular case, it can be checked that v is uniquely defined by its values at the four vertices of K, which can be chosen as the degrees of freedom for V_h.

Discretisation of the variational formulation

For simplicity, assume Ω is a polynomial domain. Let T_h be the triangulation of Ω, consisting of K_i nonoverlapping triangles, $i = 1, 2, \ldots, m$,

$$\Omega = \bigcup_{K \in T_h} K = K_1 \cup K_2 \cup \cdots \cup K_m$$

The triangles are defined such that no vertex of a triangle lies in the interior of an edge of another triangle. Before introducing the finite element space V_h, we define the mesh parameter h. For $K \in T_h$,

$$h = \max_{K \in T_h} \operatorname{diam}(K) \qquad \text{where} \qquad \operatorname{diam}(K) = \text{longest edge of } K.$$

The finite element space V_h, and $V_h \subset V$, is then introduced,

$$V_h = \Big\{v :\ v \text{ is a continuous funtion on } \Omega,\ v \in P_1(K),\ v = 0 \text{ on } \Gamma\Big\}.$$

From this, the discrete version of the variational formulation (4.7) can be formulated:

$$\text{Find } u_h \in V_h \text{ such that } a(u_h, v) = (f, v) \qquad \forall\ v \in V_h. \tag{4.8}$$

Equation (4.8) is the Galerkin finite element method for the original problem (4.1).

Basis functions

In order to obtain a system of equations written by matrix notation for the problem in question, the basis functions $\phi_i(\mathbf{x}_j)$ must be defined. Then an expression for the test functions v and the right hand side of the problem in terms of the basis functions can be found. Consequently, the matrix expression $\mathbf{Au} = \mathbf{f}$ is obtained where $\mathbf{A}$ is the stiffness matrix, $\mathbf{f}$ is the source vector and $\mathbf{u}$ is the solution vector.

The vertices, or nodes, of the triangles are denoted by $\mathbf{x}_j$, $j = 1, 2, \ldots, N$. We define the basis functions ϕ_i, $i = 1, 2, \ldots, N$, in V_h by

$$\phi_i(\mathbf{x}_j) = \begin{cases} 1 & \text{if } i = j, \\ 0 & \text{if } i \neq j. \end{cases}$$

The set of $\mathbf{x}$ where $\phi_i(\mathbf{x}_j) \neq 0$, is the support of ϕ_i and consists of the triangles with common node $\mathbf{x}_j$. Using the expression for the basis functions, we get the unique representation for the test functions,

$$v(\mathbf{x}) = \sum_{i=1}^{N} v_i \phi_i(\mathbf{x}), \qquad \mathbf{x} \in \Omega,$$

where $v_i = v(\mathbf{x}_i)$.

Matrix notation

As a result of the representation obtained for the test functions by using the basis functions, the variational formulation (4.8) can be expressed as a linear system of equations. For each j, set $v = \phi_j$ in (4.8)

$$a(u_h, \phi_j) = (f, \phi_j), \qquad j = 1, 2, \ldots, N. \tag{4.9}$$

Let

$$u_h = \sum_{i=1}^{N} u_i \phi_i, \qquad u_i = u_h(\mathbf{x}_i),$$

and insert this in (4.9) to obtain the linear system of equations

$$\sum_{1=1}^{N} a(\phi_i, \phi_j)\xi_i = (f, \phi_j), \qquad j = 1, 2, \ldots, N. \tag{4.10}$$

Written in matrix form, we have

$$\mathbf{Au} = \mathbf{f}, \tag{4.11}$$

where the stiffness matrix $\mathbf{A}$, the solution vector $\mathbf{u}$ and the source vector $\mathbf{f}$ are given by

$$\mathbf{A} = \begin{pmatrix} a_{11} & a_{12} & \dots & a_{1N} \\ a_{21} & a_{22} & \dots & a_{2N} \\ \vdots & \vdots & \ddots & \vdots \\ a_{N1} & a_{N2} & \dots & a_{NN} \end{pmatrix}, \quad \mathbf{u} = \begin{pmatrix} u_1 \\ u_2 \\ \vdots \\ u_N \end{pmatrix}, \quad \mathbf{f} = \begin{pmatrix} f_1 \\ f_2 \\ \vdots \\ f_N \end{pmatrix},$$

with

$$a_{ij} = a(\phi_i, \phi_j), \qquad f_j = (f, \phi_j), \qquad i, j = 1, 2, \dots, N.$$

The matrix $\mathbf{A}$ is symmetric and positive definite. It is also nonsingular, hence the linear system (4.11) and thus the Galerkin finite element method (4.8) have a unique solution.

To illustrate the shape of the stiffness matrix $\mathbf{A}$, consider the domain $\Omega = (0,1) \times (0,1)$. For the four corner nodes on the boundary of the domain, there will only be three nonzeros in the row. There will be at most five nonzeros per row for the internal nodes. The matrix $\mathbf{A}$ has the form:

$$\mathbf{A} = \begin{pmatrix} 4 & -1 & 0 & 0 & \dots & 0 & -1 & 0 & \dots & 0 & 0 \\ -1 & 4 & -1 & 0 & \dots & 0 & 0 & -1 & \dots & 0 & 0 \\ 0 & -1 & 4 & -1 & \dots & 0 & 0 & 0 & \dots & -1 & 0 \\ 0 & 0 & -1 & 4 & \dots & 0 & 0 & 0 & \dots & 0 & -1 \\ \vdots & \vdots & \vdots & \vdots & \ddots & \vdots & \vdots & \vdots & \ddots & \vdots & \vdots \\ 0 & 0 & 0 & 0 & \dots & 4 & -1 & 0 & \dots & 0 & 0 \\ -1 & 0 & 0 & 0 & \dots & -1 & 4 & -1 & \dots & 0 & 0 \\ 0 & -1 & 0 & 0 & \dots & 0 & -1 & 4 & \dots & 0 & 0 \\ \vdots & \vdots & \vdots & \vdots & \ddots & \vdots & \vdots & \vdots & \ddots & \vdots & \vdots \\ 0 & 0 & -1 & 0 & \dots & 0 & 0 & 0 & \dots & 4 & -1 \\ 0 & 0 & 0 & -1 & \dots & 0 & 0 & 0 & \dots & -1 & 4 \end{pmatrix}.$$

The pattern within the matrix can be reformulated or expressed by a 5-point stencil scheme obtained when dividing (4.11) by h^2.

4.1.3 Extension to general boundary conditions

There are primarily four different kinds of boundary conditions; first, second, third and fourth kind of boundary conditions. Consider the stationary problem

$$\begin{aligned} -\Delta u &= f \qquad \text{on } \Omega, \\ bu + \frac{\partial u}{\partial \nu} &= g \qquad \text{on } \Gamma, \end{aligned} \tag{4.12}$$

where b and g are given functions, and $\frac{\partial u}{\partial \nu}$ is the outward normal derivative. When the coefficient b is infinity, a first kind or Dirichlet boundary condition is imposed, whilst setting $b = 0$ gives the second kind or Neumann boundary condition. We will evaluate this problem having the function b bounded. Hence, a third kind

of boundary conditions is imposed. The fourth kind of boundary condition is a periodic boundary condition, for instance $u(0, x_2, t) = u(1, x_2, t)$ or $\frac{\partial u}{\partial x_1}(0, x_2, t) = \frac{\partial u}{\partial x_1}(1, x_2, t)$.

As in the previous section, a linear space

$$V = \Big\{ v : \ v \text{ is a continuous funtion on } \Omega, \\ \frac{\partial v}{\partial x_1} \text{ and } \frac{\partial v}{\partial x_2} \text{ are piecewise continuous and bounded on } \Omega \Big\},$$

and the following notations

$$a(u, v) = \int_\Omega \nabla u \cdot \nabla v \ d\Omega + \int_\Gamma buv \ d\Gamma, \qquad u, v \in V,$$

$$(f, v) = \int_\Omega fv \ d\Omega, \qquad v \in V,$$

$$(g, v)_\Gamma = \int_\Gamma gv \ d\Gamma, \qquad v \in V,$$

are introduced to establish the variational formulation:

$$\text{Find } u \in V \text{ such that } a(u, v) = (f, v) + (g, v)_\Gamma \qquad \forall v \in V. \tag{4.13}$$

For the stationary problem (4.1) considered in Section 4.1.1, the boundary condition was imposed in the linear space V, while in the variational formulation (4.13), the boundary condition appears implicitly. When the boundary conditions must be imposed, either explicitly in V or implicitly as in the variational formulation, we call them essential conditions. A natural condition is a boundary condition that need not to be imposed. Dirichlet boundary conditions are essential conditions, while a pure Neumann boundary condition is termed a natural condition.

There are some special cases that need to be discussed when considering general boundary conditions. If the function $b = 0$ on Γ, then the divergence theorem in the plane applied on the stationary problem (4.12) gives

$$\int_\Omega f \ d\Omega + \int_\Gamma g \ d\Gamma = 0. \tag{4.14}$$

This is a compatibility condition that must be satisfied for the stationary problem (4.12) to have a solution. In this case, u is uniquely up to an additive constant. This has to be taken into account in the definition of V. A proper modification of V could be:

$$V = \Big\{ v : \ v \text{ is a continuous function on } \Omega, \\ \frac{\partial v}{\partial x_1} \text{ and } \frac{\partial v}{\partial x_2} \text{ are piecewise continuous and bounded on } \Omega, \text{ and } \int_\Omega v \ d\Omega = 0 \Big\}.$$

We then can construct the finite element method for the stationary problem (4.12) by letting T_h be the triangulation of Ω. The finite element space V_h is then

$$V_h = \Big\{ v : \ v \text{ is a continuous function on } \Omega, \ v \in P_1(K), \ K \in T_h \Big\}.$$

The functions in V_h is not required to satisfy any boundary conditions. However, if pure Neumann boundary conditions are considered, a modification of V_h is needed:

$$V_h = \Big\{ v : \ v \text{ is a continuous function on } \Omega, \ v \in P_1(K), \ K \in T_h, \text{ and } \int_\Omega v \, d\Omega = 0 \Big\}.$$

The discrete variational formulation can then be obtained:

$$\text{Find } u_h \in V_h \text{ such that } a(u_h, v) = (f, v) + (g, v)_\Gamma \qquad \forall v \in V_h. \tag{4.15}$$

In the case of periodic boundary conditions, assume that the functions in equation evaluated, that is, problem (4.12), are spatially Ω-periodic. The linear space V must accordingly be modified to

$$\begin{aligned} V = \Big\{ & v : \ v \text{ is a continuous function on } \Omega \text{ and } \Omega\text{-periodic}, \\ & \frac{\partial v}{\partial x_1} \text{ and } \frac{\partial v}{\partial x_2} \text{ are piecewise continious and bounded on } \Omega \Big\}. \end{aligned}$$

This leads to a modification of the space V_h as well, but the variational formulations obtained in the analysis above remain unchanged [6].

4.1.4 General domains

Up to now, we have assumed the domain Ω being polygonal. If Ω is a curved domain, a transformation or mapping between the elements in the domain to a parent domain, or reference domain, is needed as the elements in the partition of the domain may no longer be uniform and have straight lines between the nodes. The angles may also differ from element to element.

If we let the finite element be $(\hat{K}, P(\hat{K}), \sum_{\hat{K}})$ where $\hat{K}$ is the reference element, $P(\hat{K})$ is the finite dimensional linear space of functions on $\hat{K}$, and $\sum_{\hat{K}}$ is the corresponding set of degrees of freedom such that functions $v \in P(\hat{K})$ are uniquely defined by $\sum_{\hat{K}}$.For Lagrangian type of elements, all degrees of freedom are defined by the function values at certain points $\hat{m}_i$, $i = 1, 2, \ldots, l$. Suppose $\mathbf{F}$ is a one-to-one mapping of $\hat{K}$ onto a curved element K in the $\mathbf{x}$-plane with inverse $\mathbf{F}^{-1}$, i.e. $K = F(\hat{K})$. We then define

$$P(K) = \{ v \ : \ v(\mathbf{x}) = v(\mathbf{F}^{-1}(\mathbf{x})), \ \mathbf{x} \in \mathbf{K}, \hat{v} \in P(\hat{K}) \}$$

$$\sum_K \text{ consists of function values at } \mathbf{m}_i = \mathbf{F}(\hat{m}_i), \ i = 1, 2, \ldots, l.$$

If $\mathbf{F} = (F_1, F_2)$ is the same type of functions in $P(K)$, i.e. $F_1, F_2 \in P(K)$, then we say that the element $(K, P(K), \sum_K)$ is an isoparametric element. In general, $\mathbf{F}^{-1}$ is not a polynomial, hence the functions $v \in P(\mathbf{K})$ are not polynomials.

For the partitioning $K_h = \{K\}$ of Ω, K may have at least one curved edge. Let $\Omega_h = \cup_{K_c \in T_h} K_c$ where K_c are elements with at least one curved edge and Ω_h is an approximation of Ω with piecewise smooth boundary. An appropriate finite element space will then be

$$V = \Big\{ v : \ v \text{ is a continuous function on } \Omega, \ v|_K \in P_1(K), \ K \in T_h \Big\}.$$

Consider the problem presented in Section 4.1.1, Equation (4.1), the finite element method obtained was:

$$\text{Find } u_h \in V_h \text{ such that } a(u_h) = (f, v). \tag{4.16}$$

Let $\{\phi_i\}_{i=1}^{l}$ be the basis of $P(\hat{K})$. Define $\phi_i(\mathbf{x}) = \hat{\phi}_i(\mathbf{F}^{-1}(\mathbf{x}))$, $\mathbf{x} \in \mathbf{K}$, $i = 1, 2, \ldots, l$. We need to compute

$$a_K(\phi_i, \phi_j) = \int_K \nabla\phi_i \cdot \nabla\phi_j \ d\Omega, \qquad i, j = 1, 2. \ldots, l,$$

and

$$\frac{\partial \phi_i}{\partial x_k} = \frac{\partial}{\partial x_k}(\hat{\phi}_i(\mathbf{F}^{-1}(\mathbf{x}))) = \frac{\partial \hat{\phi}_i}{\partial \hat{x}_1}\frac{\partial \hat{x}_1}{\partial x_k} + \frac{\partial \hat{\phi}_i}{\partial \hat{x}_2}\frac{\partial \hat{x}_2}{\partial x_k}$$

for $k = 1, 2$. Then $\nabla\phi_i$ can be expressed by the Jacobian of $\mathbf{F}^{-1}$, $\mathbf{J}^{-T}$, as

$$\nabla\phi_i = \mathbf{J}^{-T}\nabla\hat{\phi}_i,$$

where

$$\mathbf{J}^{-T} = \begin{pmatrix} \frac{\partial \hat{x}_1}{\partial x_1} & \frac{\partial \hat{x}_2}{\partial x_1} \\ \frac{\partial \hat{x}_1}{\partial x_2} & \frac{\partial \hat{x}_2}{\partial x_2} \end{pmatrix}.$$

We then have to apply the change of variable $F : \ \hat{K} \to K$ in order to transform the values computed for the reference element to the elements in the partition of the domain. Hence, we obtain

$$a_K(\phi_i, \phi_j) = \int_{\hat{K}} (\mathbf{J}^{-T}\nabla\hat{\phi}_i) \cdot (\mathbf{J}^{-T}\nabla\hat{\phi}_j)|\det \mathbf{J}| \ d\hat{\Omega}, \qquad \text{for } i, j = 1, 2, \ldots, l,$$

where $|\det \mathbf{J}|$ is the value of the determinant of the Jacobian $\mathbf{J}$,

$$\mathbf{J} = \begin{pmatrix} \frac{\partial x_1}{\partial \hat{x}_1} & \frac{\partial x_1}{\partial \hat{x}_2} \\ \frac{\partial x_2}{\partial \hat{x}_1} & \frac{\partial x_2}{\partial \hat{x}_2} \end{pmatrix}.$$

From linear algebra we get

$$\mathbf{J}^{-T} = (\mathbf{J}^{-1})^T = \frac{1}{|\det \mathbf{J}|}\mathbf{J}',$$

where

$$\mathbf{J}' = \begin{pmatrix} \frac{\partial x_2}{\partial \hat{x}_2} & -\frac{\partial x_2}{\partial \hat{x}_1} \\ -\frac{\partial x_1}{\partial \hat{x}_2} & \frac{\partial x_1}{\partial \hat{x}_1} \end{pmatrix}.$$

Thus,

$$a_K(\phi_i, \phi_j) = \int_{\hat{K}} (\mathbf{J}'\nabla\phi_i) \cdot (\mathbf{J}'\nabla\phi_j) \frac{1}{|\det \mathbf{J}|}\, d\hat{\Omega}, \qquad \text{for } i, j = 1, 2, \ldots, l.$$

These integrals are in general difficult to evaluate, and we therefore need a numerical integration formula for solving this kind of integrals.

Quadrature rules

The theory presented above, applies for partitions of both triangles and rectangles. As quadrilateral elements are used in the numerical modelling tool presented in Chapter 5, quadrature rules will only be discussed for quadrilateral elements.

For simplicity, we will consider the function $f : \Omega_h \subset \mathbb{R}^n \to \mathbb{R}$, where f is assumed to be smooth and integrable and n is the number of space dimensions. The integral of interest is then

$$\int_{\Omega_h} f(\mathbf{x})\, d\Omega,$$

and $f(\mathbf{x})$ can be thought of as the integrand of the stiffness matrix. Using the change of variables formula, the one-dimensional case can be represented as

$$\int_{\Omega_h} f(x)\, dx = \int_{-1}^{1} f(x(\xi)) \frac{\partial x}{\partial \xi}(\xi)\, d\xi.$$

In two dimensions the change of variables formula give the following

$$\int_{\Omega_h} f(x_1, x_2)\, d\Omega = \int_{-1}^{1}\int_{-1}^{1} f(x_1(\xi,\eta), x_2(\xi,\eta))|\det \mathbf{J}(\xi,\eta)|\, d\xi d\eta,$$

where $\mathbf{J}(\xi, \eta)$ is the Jacobian. In the general case

$$\int_{\Omega_h} f(\mathbf{x})\, d\Omega = \int_{K} f(\mathbf{x}(\xi))|\det \mathbf{J}(\boldsymbol{\xi})|\, d\boldsymbol{\xi},$$

for $\mathbf{x} = (x_1, x_2, \ldots, n)$ and $\boldsymbol{\xi} = \xi_1, \xi_2, \ldots, n$ for n integrals.

Consider the one-dimension case where the integral

$$\int_{-1}^{1} g(\xi)\ d\xi$$

is the one to be evaluated. This integral can be approximately computed by a numerical integration (quadrature) formula as follows

$$\int_{-1}^{1} g(\xi)\ d\xi = \sum_{l=1}^{m} g(\tilde{\xi}_l)W_l + R \cong \sum_{l=1}^{m} g(\tilde{\xi}_l)W_l, \tag{4.17}$$

where m is the number of integration (quadrature) points, $\tilde{\xi}_l$ is the coordinate of the lth integration point, W_l is the weight of the lth integration point, and R is the remainder. Widely known integration formulas are the classical ones as the trapezoidal rule and Simpson's rule. However, these methods are inefficient in the sense that there exists methods that require fewer integration points but are just as accurate. This is in practise of great importance since the fewer integration points, the less the cost and considerable savings can be obtained by choosing an appropriate numerical integration rule.

Gaussian quadrature

The Gaussian quadrature formulas are optimal in one dimension. Accuracy of order $2m$ is achieved by m integration points, and the locations of the integration points and values of associated weights are determined to attain maximum accuracy [9], [10]. The first three Gaussian quadrature rules can be presented as follows; see, for instance Hughes [9]:

1. For one integration point, $m = 1$:

$$\tilde{\xi}_1 = 0, \qquad W_1 = 2, \qquad R = \frac{g^{(2)}(\tilde{\xi})}{3}.$$

2. For two integration points, $m = 2$:

$$\tilde{\xi}_1 = \frac{-1}{\sqrt{3}}, \qquad \tilde{\xi}_2 = \frac{1}{\sqrt{3}}, \qquad W_1 = W_2 = 1, \qquad R = \frac{g^{(4)}(\tilde{\xi})}{135}.$$

3. For three integration points, $m = 3$:

$$\tilde{\xi}_1 = -\sqrt{\frac{3}{5}}, \quad \tilde{\xi}_2 = 0, \quad \tilde{\xi}_3 = \sqrt{\frac{3}{5}}, \quad W_1 = W_3 = \frac{5}{9}, \qquad W_2 = \frac{8}{9}, \quad R = \frac{g^{(6)}(\tilde{\xi})}{15750}.$$

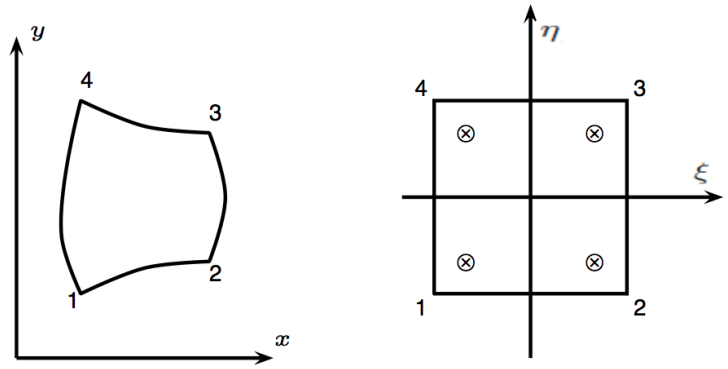

Figure 4.1: Mapping of quadrilateral elements with a 4-point Gaussian quadrature rule. Each of the quadrature points is marked by a cross.

In the above expressions,

$$g^{(2)} = \frac{\partial^2 g(\tilde{\xi})}{\partial \tilde{\xi}^2}. \tag{4.18}$$

The mapping of quadrilateral elements with a 4-point Gaussian quadrature rule is shown in Figure 4.1, where the Gaussian quadrature points are marked by crosses.

The theory of Gaussian quadrature formulas is thoroughly discussed by Stroud and Secrest in [10]. See Hughes [9] or Stroud and Secrest [10] for the general Gaussian quadrature rule.

For integrals in several dimensions, Gaussian quadrature rules are constructed by applying one-dimensional Gaussian rules on each coordinate separately. Hence, the Gaussian quadrature rule in two dimensions is as follows

$$\int_1^1 \int_1^1 g(\xi, \eta)\ d\xi d\eta \cong \sum_{l^{(1)}=1}^{m^{(1)}} \sum_{l^{(2)}=1}^{m^{(2)}} g(\tilde{\xi}^{(1)}_{l^{(1)}}, \tilde{\eta}^{(2)}_{l^{(2)}}) W^{(1)}_{l^{(1)}} W^{(2)}_{l^{(2)}}. \tag{4.19}$$

4.2 Finite element methods for transient problems

The model equations considered in Chapter 2 form a transient (parabolic) problem. Depending on the dominating processes, the character of the problem can either be parabolic or hyperbolic. When evaluating parabolic problems for two-phase or multiphase flow in porous media, the equations in general have hyperbolic character. That is, the parabolic term in the equation is small compared to the hyperbolic term, and hence, the effect of the parabolic term to the properties of the equation is negligible. However, in the case of natural convection, the parabolic term is not negligible and hence, the problem is of parabolic character.

In Chapter 3, the dimensionless equivalent of the model equations were presented.

A general form of the model equations for energy is

$$\frac{\partial u}{\partial t} + \mathbf{v} \cdot \ \nabla u \ - \nabla \cdot (\kappa \nabla u) + \sigma u = q. \tag{4.20}$$

This general form of the equations will be used when discussing the finite element method for transient problems. The rate of change of the quantity u is due to the advection term $\mathbf{v} \cdot \nabla u$, the diffusion term $\nabla \cdot (\kappa \nabla u)$, generative forces in σu and sources and sinks expressed by q. Thus, in this section the following problem in a bounded domain $\Omega \subset \mathbb{R}^d$, $d \geq 1$ will be evaluated:

$$\left.\begin{aligned} \frac{\partial u}{\partial t} + \mathbf{v} \cdot \ \nabla u \ - \nabla \cdot (\kappa \nabla u) + \sigma u = q \qquad & \text{in } \Omega \times J, \\ u = 0 \qquad & \text{on } \Gamma \times J, \end{aligned}\right\} \tag{4.21}$$

where J is the time interval, $J = (0, T)$ with $T > 0$. The initial condition $u(\cdot, 0) = u_0$ in Ω is also imposed.

4.2.1 A semidiscrete scheme in space

First we will present an approximation scheme where the problem is only discretised in space using the finite element method. This is called a semidiscrete approximation scheme. We search for a solution within the space

$$\begin{aligned} V = \Big\{ v : \ & v \text{ is a continuous function on } \Omega, \\ & \frac{\partial v}{\partial x_1} \text{ and } \frac{\partial v}{\partial x_2} \text{ are piecewise continuous and bounded on } \Omega, \ v|_\Gamma = 0 \Big\}. \end{aligned}$$

We introduce a similar notation as in Section 4.1.1,

$$a(u, v) = \int_\Omega \kappa \ \nabla u \ \cdot \ \nabla v \ \ d\Omega, \qquad (q, v) = \int_\Omega qv \ d\Omega,$$

but also include

$$c(u, v) = \int_\Omega \mathbf{v} \cdot \ \nabla u \ v \ d\Omega, \qquad (\sigma u, v) = \int_\Omega \sigma u v \ d\Omega,$$

in order to write the problem on variational form: Find $u : J \to V$ such that

$$\begin{aligned} \Big(\frac{\partial u}{\partial t}, v\Big) + c(u, v) - a(u, v) + (\sigma u, v) = (q, v) \qquad & \forall \ v \in V, \ t \in J, \\ u(\mathbf{x}, 0) = u_0(\mathbf{x}) \qquad & \forall \ \mathbf{x} \in \Omega. \end{aligned} \tag{4.22}$$

Let V_h be a finite element subspace of V. A semidiscrete version of the variational formulation can then be found: Find $u_h : J \to V_h$ such that

$$\begin{aligned} \Big(\frac{\partial u_h}{\partial t}, v\Big) + c(u_h, v) - a(u_h, v) + (\sigma u_h, v) = (q, v) \qquad & \forall \ v \in V_h, \ t \in J, \\ (u_h(\cdot, 0), v) = (u_0, v) \qquad & \forall \ v \in V_h. \end{aligned} \tag{4.23}$$

This is a semidiscrete system as u is discretised in space but not in time. Again we let the basis functions be denoted by ϕ_i, $i = 1, 2, \ldots, N$, $\phi_i \in V_h$. Then u_h can be expressed in terms of the basis functions,

$$u_h(\mathbf{x}, t) = \sum_{i=1}^{N} u_i(t)\phi_i(\mathbf{x}) \qquad (\mathbf{x}, t) \in \Omega \times J, \tag{4.24}$$

where $u_i = u_h(x_i)$. For $j = 1, 2, \ldots, N$, $v = \phi_j$ inserted in (4.23) applied with (4.24) such that for $t \in J$,

$$\sum_{i=1}^{N}(\phi_i, \phi_j)\frac{\partial u_i}{\partial t} + \sum_{i=1}^{N} c(\phi_i, \phi_j)u_i - \sum_{i=1}^{N} a(\phi_i, \phi_j)u_i + \sum_{i=1}^{N}(\phi_i, \phi_j)\sigma u_i = (q, \phi_j), \quad j = 1, 2, \ldots, M,$$
$$\sum_{i=1}^{N}(\phi_i, \phi_j)u_i(0) = (u_0, \phi_j), \quad j = 1, 2, \ldots, M.$$

Expressed in matrix form, we get

$$\begin{aligned} \mathbf{B}\frac{\partial \mathbf{u}(t)}{\partial t} + \mathbf{C}\mathbf{u}(t) - \mathbf{A}\mathbf{u}(t) + \sigma\mathbf{B}\mathbf{u}(t) &= \mathbf{q}(t), \\ \mathbf{B}\mathbf{u}(0) &= \mathbf{u}_0, \end{aligned} \tag{4.25}$$

where

$$\begin{aligned} \mathbf{A} &= \{a_{ij}\}, \qquad a_{ij} = a(\phi_i, \phi_j), \\ \mathbf{B} &= \{b_{ij}\}, \qquad b_{ij} = (\phi_i, \phi_j), \\ \mathbf{C} &= \{c_{ij}\}, \qquad c_{ij} = c(\phi_i, \phi_j), \\ \mathbf{u} &= \{u_j\}, \quad \mathbf{q} = \{q_j\}, \quad q_j = (q, \phi_j). \end{aligned}$$

4.2.2 Fully discrete schemes

In order to find a finite element method for the transient problem (4.21), we have to discretise u in time and obtain a fully discrete scheme.

Time discretisation: The θ-family of methods

There are several different ways for discretising the time derivative, like the Lax-Wendroff method, the leap-frog method and the θ-family of methods [11]. Both the Lax-Wendroff and the leap-frog method are second order accurate time-stepping methods. The order of accuracy for the θ-family of methods depends on the choice of θ.

The θ-family of methods is a single step method widely used for integrating first-order differential equations. In this method, the value u^{n+1} of the solution variable at time $t^{n+1} = t^n + \Delta t$ is determined from the value u^n at time t^n by a weighted average of u_t^n and u_t^{n+1} at the end points of the integration step:

$$\frac{u(t^{n+1}) - u(t^n)}{\Delta t} = \theta u_t(t^{n+1}) + (1 - \theta)u_t(t^n) + \mathcal{O}((1/2 - \theta)\Delta t, \Delta t^2), \tag{4.26}$$

where Δt is the time step and $\theta \in [0,1]$. By different choices of the parameter θ, several well-known methods are obtained. For $\theta < 1/2$, the methods are conditionally stable, while choices of θ in the interval $[1/2, 1]$ gives unconditionally stable methods [6,11]. Setting $\theta = 0$ gives the forward Euler method, while $\theta = 1$ gives the backward Euler method and the trapezoidal rule is obtained when $\theta = 1/2$. When the trapezoidal rule is used, the resulting method is the Crank-Nicholson method. The methods obtained for $\theta = 0, 1$ are first-order accurate in time, while $\theta = 1/2$ gives a second-order accurate time-stepping method.

(i) The backward Euler method

Let $0 = t^0 < t^1 < \cdots < t^N = T$ be a partition of J. Then J is divided into N subintervals, $J^n = (t^{n-1}, t^n)$ with length $\Delta t^n = t^n - t^{n-1}$. For a generic function v of time, set $v^n = v(t^n)$. The backward Euler method for the semidiscrete version of the problem (4.23) appear by writing Equation (4.26) on variational form, and replacing $(\frac{\partial u}{\partial t}, v)$ in Equation (4.22) by the this expression. Hence, the backward Euler method for the semidiscrete version of the problem (4.23) is: Find $u_h \in V_h$, $n = 1, 2, \ldots, N$ such that

$$\begin{aligned} \Big(\frac{u_h^n - u_h^{n-1}}{\Delta t^n}, v\Big) + c(u_h^n, v) - a(u_h^n, v) + (\sigma u_h^n, v) &= (q^n, v) \qquad \forall\ v \in V_h, \\ (u_h^0, v) &= (u_0, v) \qquad \forall\ v \in V_h. \end{aligned} \tag{4.27}$$

This procedure results in a discretisation error of order $\mathcal{O}(\Delta t^n)$. On matrix form:

$$\begin{aligned} (\mathbf{B} + \mathbf{A}\Delta t^n + \sigma\mathbf{B} + \mathbf{C}\Delta t^n)\mathbf{u}^n &= \mathbf{B}\mathbf{u}^{n-1} + \mathbf{q}^n \Delta t^n, \\ \mathbf{B}\mathbf{u}(0) &= \mathbf{u}_0, \end{aligned} \tag{4.28}$$

where $u_h^n = \sum_{i=1}^M u_i^n \phi_i$, $n = 0, 1, \ldots, N$, and $\mathbf{u}^n = (u_1^n, u_2^n, \ldots, u_M^n)^T$. This an implicit scheme.

We will now look more into the stability of this scheme. We assume q, σ and $\mathbf{v}$ are all zero for simplicity. The matrix equation can then be formulated as

$$(\mathbf{B} + \mathbf{A}\Delta t^n)\mathbf{u}^n = \mathbf{B}\mathbf{u}^{n-1}. \tag{4.29}$$

Choosing $v = u_h^n$ and inserting this in (4.27), we observe that the following expression can be obtained

$$\|u_h^n\|^2 - (u_h^{n-1}, u_h^n) - a(u_h^n, u_h^n)\Delta t^n = 0.$$

Cauchy's inequality, $|(v, w)| \leq \|v\|\|w\|$, yields the following

$$(u_h^{n-1}, u_h^n) \leq \|u_h^{n-1}\|\|u_h^n\| \leq \frac{1}{2}\|u_h^{n-1}\|^2 + \frac{1}{2}\|u_h^n\|^2.$$

By rearranging, the expression

$$\frac{1}{2}\|u_h^n\|^2 - \frac{1}{2}\|u_h^{n-1}\|^2 + a(u_h^n, u_h^n)\Delta t^n \leq 0,$$

appears. Summing over n and using $(u_h^0, v) = (u_0, v)$ gives,

$$\|u_h^j\|^2 + 2\sum_{n=1}^{j} a(u_h^n, u_h^n)\Delta t^n \leq \|u_h^0\|^2 \leq \|u^0\|^2.$$

As $a(u_h^n, u_h^n) \geq 0$ gives

$$\|u_h^j\| \leq \|u_h^0\|, \qquad j = 0, 1, \ldots, n, \tag{4.30}$$

and this proves that the backward Euler method is unconditionally stable as this stability result (4.30) is independent of Δt^n.

(ii) The forward Euler method

We use the same partition of J as for the backward Euler method. The forward Euler method for the semidiscrete version of the problem (4.23) is then: Find $u_h^n \in V_h$, $n = 1, 2, \ldots, N$ such that

$$\begin{aligned} \Big(\frac{u_h^n - u_h^{n-1}}{\Delta t^n}, v\Big) + c(u_h^{n-1}, v) - a(u_h^{n-1}, v) + (\sigma u_h^{n-1}, v) &= (q^{n-1}, v) \qquad \forall\, v \in V_h, \\ (u_h^0, v) &= (u_0, v) \qquad \forall\, v \in V_h. \end{aligned} \tag{4.31}$$

On matrix form, this is

$$\begin{aligned} \mathbf{B}\mathbf{u}^n = (\mathbf{B} - \mathbf{C}\Delta t^n + \mathbf{A}\Delta t^n - \sigma\mathbf{B}\Delta t)\mathbf{u}^{n-1} + \mathbf{q}^{n-1}\Delta t^n, \\ \mathbf{B}\mathbf{u}(0) = \mathbf{u}_0. \end{aligned} \tag{4.32}$$

This is an explicit scheme, and hence is unconditionally stable [6, 12].

(iii) The trapezoidal rule

The third method we will discuss, is the trapezoidal rule. The time interval J is partitioned as for the two other methods. The trapezoidal rule for (4.23) is: Find $u_h \in V_h$, $n = 1, 2, \ldots, N$ such that $\forall\, v \in V_h$,

$$\begin{aligned} \Big(\frac{u_h^n - u_h^{n-1}}{\Delta t^n}, v\Big) + c(\frac{u_h^n + u_h^{n-1}}{2}, v) - a(\frac{u_h^n + u_h^{n-1}}{2}, v) + (\sigma\frac{u_h^n + u_h^{n-1}}{2}, v) &= (\frac{q^n + q^{n-1}}{2}, v), \\ (u_h^0, v) &= (u_0, v). \end{aligned} \tag{4.33}$$

The trapezoidal on matrix form:

$$(\mathbf{B}+\mathbf{C}\frac{\Delta t^n}{2}-\mathbf{A}\frac{\Delta t^n}{2}+\sigma\mathbf{B}\frac{\Delta t^n}{2})\mathbf{u^n} = (\mathbf{B}+\mathbf{C}\frac{\Delta t^n}{2}-\mathbf{A}\frac{\Delta t^n}{2}+\sigma\mathbf{B}\frac{\Delta t^n}{2})\mathbf{u^{n-1}}+\frac{\mathbf{q^n}+\mathbf{q^{n-1}}}{2}\Delta t^n, \tag{4.34}$$

for $n = 1, 2, \ldots, N$. Setting σ, q and $\mathbf{v}$ as zero for simplicity and inserting $v = \frac{u_h^n + u_h^{n-1}}{2}$, we see that this implicit method is unconditionally stable.

From the analysis above, we see that the backward Euler and the trapezoidal rule are both implicit methods that are unconditionally stable. Compared to the explicit one, forward Euler, they require more work per time step. However, the backward Euler method and the trapezoidal rule are more efficient for parabolic problems than the forward Euler method as the extra cost involved at each step for an implicit method is more than compensated by the fact that larger time steps can be utilized.

Stability criteria

When certain partial differential equations are solved numerically, a stability criterion in needed in order to assure convergence. For pure hyperbolic equations, the Courant-Friedrich-Lewy (CFL) condition [13] is used as such, and it is a necessary condition for convergence. However, it is not a sufficient condition in general [12]. Thus, if the condition is not validated, then the method cannot converge, but if the CFL condition is satisfied, a proper stability analysis is required to prove convergence and determine the restrictions on Δt and Δx if needed.

The CFL condition arises when explicit time-marching schemes are used in the computation of the numerical solution and limits the timestepping to be less than a certain time to ensure that the numerical solution is computed within the requested order of accuracy. The condition can be stated as follows,

$$C = \frac{||v||\Delta t}{\Delta x} \tag{4.35}$$

where v is the velocity, Δt is the length of the timestep and Δx is the length scale which for uniform grids corresponds to the length of an element. The number C is referred to as the Courant number, and

$$C \leq 1 \tag{4.36}$$

must be satisfied for stability. This is satisfied when the numerical domain of dependence contains the analytical domain of dependence as then the information required to form the solution can be accessed. In other words, if a wave is crossing a discrete grid, then the timestepping must be less than the time for the wave to travel adjacent grid points.

When the problem at hand is a pure transient diffusion problem, like the heat equation, another stability criterion is needed. It can be shown that an explicit method, for instance the forward Euler method, is stable when the condition

$$\Delta t^n \leq Ch^2, \qquad n = 1, 2, \ldots, N, \tag{4.37}$$

where C is a constant independent of the time step Δt^n and the mesh parameter h, is satisfied. This is a very restrictive criterion, especially for long-time integration [11].

Problems on the form as the general model equation for energy, Equation (4.20), is a complex problem where both parabolic and hyperbolic terms are present. When applying explicit schemes for solving this kind of problem, both criteria mentioned, (4.37,4.35), must be satisfied for stability.

4.3 The SUPG method

In application to problems in solid/structural mechanics and other situations governed by diffusion-type equations, standard finite elements approximations are eminently successful [11]. This is due to the symmetric stiffness matrices that arises when the Galerkin finite element method is applied to problems governed by self-adjoint elliptic and parabolic partial differential equations. However, when applying the FEM to flow problems, the advantages of the method is no longer as significant, and especially regarding to modelling advection-dominated transport phenomena as the advection operators are nonsymmetric. Thus, the approximation property used to utilise the symmetry obtained for diffusion-type equations, is lost when advection dominates the transport process.

In this section, a short introduction to the Streamline-Upwind-Petrov-Galerkin (SUPG) method will be given. The SUPG method is designed to produce stable and accurate results in the presence of highly convective effects [11].

Several techniques have been proposed to stabilise the convective term in a consistent manner such that the solution of the differential equation is also a solution of the weak form. In many of these techniques, an extra term over the element interiors is added to the Galerkin weak form. This approach is the precursor to the SUPG method, and may take this form as used by Braun in his paper [14] where he studies 3D heat transport equations solved by finite elements:

$$N^* = N + \tau \mathbf{v} \cdot B, \tag{4.38}$$

where N is the shape functions, B is the derivative of the shape functions in space, $\mathbf{v}$ is the velocity and τ is the factor applied to improve stability.

For the transient solution for pure advection problems, another approach to improve stability is presented by Tezduyar and Osawa in [15]. They proposed a τ_{SUPG}-parameter given by

$$\tau_{SUPG} = \left(\frac{1}{\tau_1^r} + \frac{1}{\tau_2^r} + \frac{1}{\tau_3^r}\right)^{-\frac{1}{r}}, \tag{4.39}$$

with

$$\tau_1 = \frac{h}{2v}, \tag{4.40}$$

$$\tau_2 = \theta \Delta t, \tag{4.41}$$

$$\tau_3 = \frac{h^2}{4\alpha} = \frac{h^2 \rho c_p}{k}. \tag{4.42}$$

The parameters τ_1, τ_2 ad τ_3 are the popular limits for the advection-dominated, the transient-dominated and the diffusion-dominated cases respectively. Common choices for r are $r = 1$ and $r = 1/2$.

In the next chapter the differences between these approaches for stabilising the advection term will be looked into when benchmarks are performed on the numerical program WAFLE.

Chapter 5

The numerical modelling tool

This chapter contains a presentation of the numerical tool, where a brief introduction of the set up and implementation of the program will be given. Limitations and advantages with the choices made while developing WAFLE will also be discussed.

5.1 WAFLE

WAFLE is a finite element based numerical program for modelling flow in geothermal systems, written in FORTRAN 90. Water would most likely be used for extracting heat from a geothermal system, and gives rise to the name of the program as WAFLE stands for WAter FLow Equations solver. WAFLE is a user-costumed program as it asks for real input values for the problem at hand. The equations are then scaled and dimensionless numbers are computed for the given set of parameters. This approach is convenient for studying real case problems, while when the behaviour of the solution for different regimes of dimensionless numbers is in question, more work from the user is demanded. The approach chosen is made as WAFLE will at a later stage be included as an extension to the pre-existing FEM-code FANTOM [1] which models plate tectonics.

5.2 Set up and implementation

5.2.1 A brief presentation of the set up of WAFLE

In the previous chapter, numerical methods for solving partial differential equations, in particular for transient problems, were discussed. When building WAFLE, linear quadrilateral elements K with bilinear polynomials

$$Q_1(K) = \{v : v(\mathbf{x}) = \sum_{i,j=0}^{1} v_{ij} x_1^i x_2^j,\ \mathbf{x} \in K,\ v_{ij} \in \mathbf{R}\},$$

are used. The corresponding finite element space is

$$V_h = \{v : v \text{ is continuous on } \Omega \text{ and } v|_K \in Q_1(K),\ K \in K_h\}.$$

Hence, the function $v \in Q_1(K)$ is bilinear,

$$v(\mathbf{x}) = v_{00} + v_{10}x_1 + v_{01}x_2 + v_{11}x_1x_2,$$

and $\mathbf{x} = (x_1, x_2) \in K$, $v_{ij} \in \mathbb{R}$, as shown in Section 4.1.2.

A flowchart of WAFLE is shown in Figure 5.1.The colours in the flowchart indicate which routines are closely related. The blue ones are all directly connected to the computation of temperature, while the pink ones deals with pressure and the light grey with velocity computations. The rest are related to general numerics, set up and post processing of data.

The first routine enables statistics and output values to be written into files for later purpose. The next two routines read the input given by the user. The user inputs real values for the geologic system in question in the input files. The reading of input values is split in two where there first routine, *read_n_compute_parameters*, handles geometry and numerics while *read_phases* deals with the material properties involved.

After the input from the user is read, a scaling of the values is performed and the further calculations are carried out in dimensionless form. This makes the tool more usable for modelling real case geologic systems. The routine *grid_setup* defines the grid and creates the arrays needed to describe the system before the porosity is set up in *porosity_setup*. The porosity ϕ is a field which can vary in space. In *assess_matrix* the matrices for solving the linear system $Ax = b$ is set up. The last two routines before the timestepping loop predefine the pressure field and the initial temperature field.

Within the timestepping loop, an iterative loop is implemented to ensure that the values obtained are of acceptable accuracy. As the equations we solve for (ref: later in this section) are coupled, one could either solve these equations simultaneously or implement an iterative loop to overcome the nonlinearities.

Within the nonlinear iterative loop there are three routines that define the boundary condition for respectively pressure, velocity and temperature: *define_bc_pres, define_bc_vel* and *define_bc_temp*. The *make_matrix*-routines perform the numerical integration on quadrature points, and compute the local matrix for each element and transfer these local matrices into the big global matrix for the whole system. The global matrix is solved in the *solve_system*-routines. The routine *compute_velocity_field*, computes the velocity field from the pressure field. Integration on quadrature points is also done in this routine.

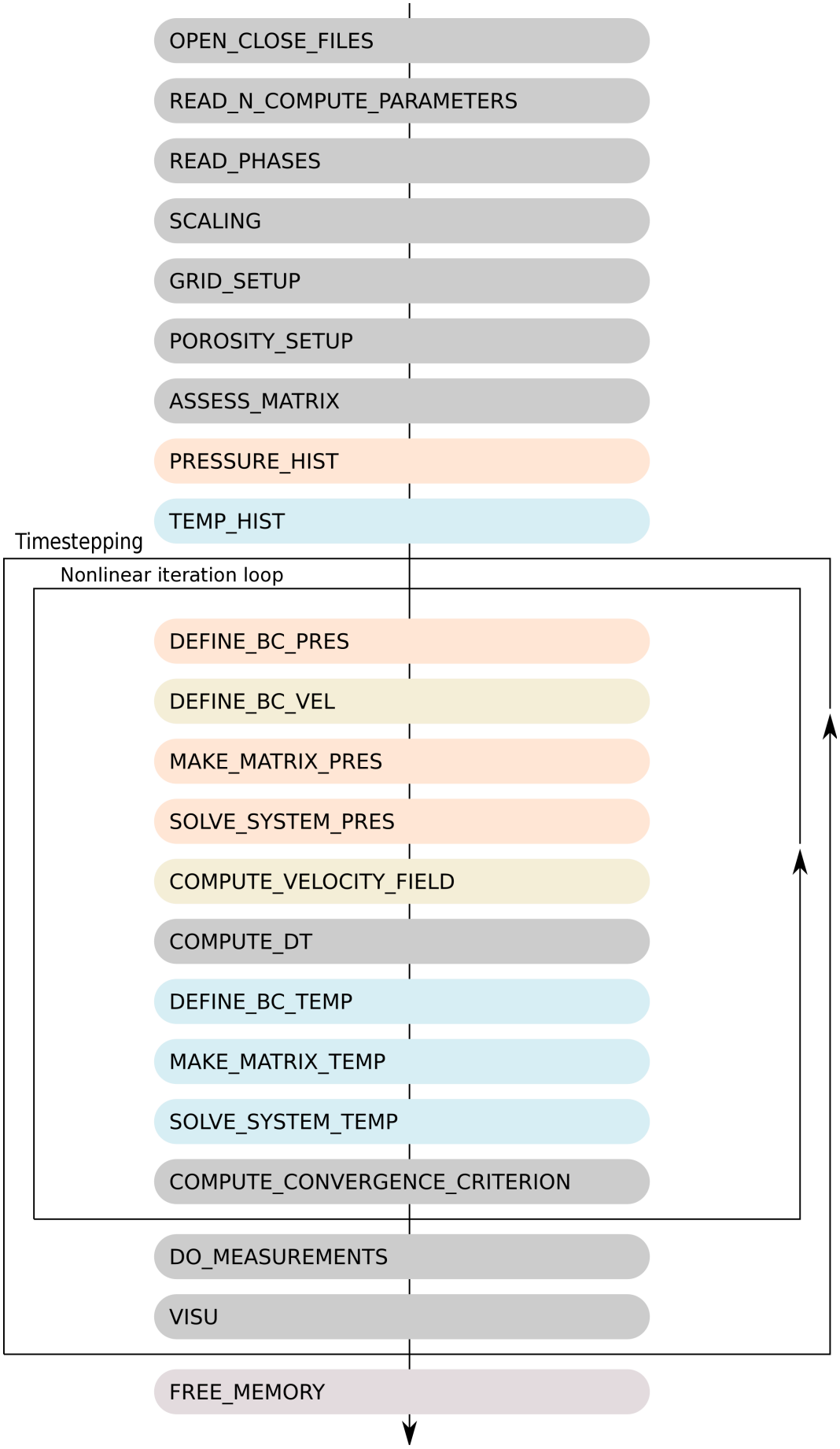

Figure 5.1: Flowchart of WAFLE.

To ensure stability, the CFL condition is implemented in *compute_dt*. Here Δt is computed for each step in the iterative loop. At the end of every nonlinear iteration, convergence criteria for pressure, velocity and temperature are computed. When all these criteria are fulfilled, we exit the nonlinear iterative loop and post process the data for the current timestep by *do_measurements* and *visu*. These routines have built-in graphics of fields and isocontours and ASCII-output of both nodal and elemental values for easy use. The name of the last routine speaks for itself; it frees the memory used when the running of WAFLE is finished.

5.3 Weak formulation

As can be seen from the flowchart, Figure 5.1, we solve first for the pressure, then recover the velocity before the temperature is computed. That is, we first solve the momentum equation (3.1) from Chapter 3

$$\mathbf{v} = -\frac{\mathbf{K}}{\mu}\left(\nabla p \ + \rho \mathbf{g}\right), \tag{5.1}$$

rewritten as

$$\nabla p = -\frac{\mu}{\mathbf{K}}\mathbf{v} - \rho \mathbf{g}, \tag{5.2}$$

where the value for $\mathbf{v}$ is from the previous iteration/ set in *define_bc_vel*. In dimensionless form, the equation can be written as

$$\nabla \hat{\mathbf{p}} = -\hat{\mathbf{v}} - RaDa\hat{T}\mathbf{k}. \tag{5.3}$$

The velocity $\mathbf{v}$ is then recovered from the pressure using the momentum equation (3.1). In dimensionless form,

$$\hat{\mathbf{v}} = -\nabla \hat{\mathbf{p}} - RaDa\hat{T}\mathbf{k}, \tag{5.4}$$

as derived in Chapter 3.

This approach has some shortcomings as computing the pressure for linear elements by the above equation, (5.3), gives a linear pressure field. The pressure is computed at the nodes of the elements, while the velocity is an elemental quantity. In this case, the velocity is a derived quantity whose accuracy is one order less than the accuracy of the pressure [16].

After the velocity is computed, we solve for the temperature for the solid and the temperature for the fluid. The energy equations were presented in Chapter 3:

$$(1-\phi)(\rho c)_s \frac{\partial T_s}{\partial t} = (1-\phi)\nabla \cdot (k_s \nabla T_s) + (1-\phi)q_s + h(T_f - T_s) \tag{5.5}$$

$$\phi(\rho c_P)_f + (\rho c_P)_f \mathbf{v} \cdot \nabla T_f = \phi \nabla \cdot (k_f \nabla T_f) + \phi q_f + h(T_s - T_f) \tag{5.6}$$

The weak formulations for the model equations above (5.2),(5.5),(5.6), can be found by the procedure described in Chapter 4. For a test function v, the weak formulation for the rewritten momentum equation is then

$$-\int_{\Omega} \nabla p \nabla v \; d\Omega - \frac{\mu}{\mathbf{K}} \int_{\Gamma} v \mathbf{v} \cdot \mathbf{n} \; d\Gamma + g \int_{\Omega} \nabla v \rho \; d\Omega = 0, \tag{5.7}$$

where $\mathbf{n}$ is the outward unit normal to Γ. The weak formulations for the energy equations for the solid and the fluid are respectively,

$$(1-\phi) \int_{\Omega} \frac{\partial T_s}{\partial t} v \; d\Omega - (1-\phi) \int_{\Omega} k_s \nabla T_s \cdot \nabla v \; d\Omega + \int_{\Omega} h T_s v \; d\Omega = \int_{\Omega} [(1-\phi) q_s + h T_f] v \; d\Omega, \tag{5.8}$$

$$(\phi) \int_{\Omega} \frac{\partial T_f}{\partial t} v \; d\Omega + (\rho c_p)_f \int_{\Omega} \mathbf{v} \cdot \nabla T_f v \; d\Omega - \phi \int_{\Omega} k_f \nabla T_f \cdot \nabla v \; d\Omega + \int_{\Omega} h T_f \; d\Omega = \int_{\Omega} (\phi q_f + h T_s) v \; d\Omega. \tag{5.9}$$

These integrals are solved by use of a 4-point Gaussian quadrature rule, and the fully discretised scheme is obtained by use of the θ-family method, choosing $\theta = 1/2$, see Chapter 4.

5.4 Solver

When using numerical methods like finite element and finite difference methods for solving problems, a coupled system of algebraic equations, $Ax = b$ where A is a matrix consisting of the coefficients in the coupled equations, x is the solution vector, and b is the right hand side vector, is obtained. Solving this system of equations is the most time-consuming part of a large scale finite element or finite difference computation, hence it is important that a proper choice for solver is made.

This choice depends on different factors like for instance, the elements used in the model, the shape of the model, the computer resources available and the type of analysis performed. Common choices would be using an iterative or a direct solver.

Direct solvers are based on a factorisation of the matrix A for solving the system $Ax = b$. The choice of the factorisation depends on the mathematical structure and the storage of A. That is, whether the matrix is Hermitian or non-Hermitian, and definite or indefinite, and whether A is banded, dense, sparse or structured. For Hermitian matrices, the factorisation is on the form $A = L^T L$, L being a lower triangular matrix, as it exploits the fact of A being symmetric. For non-Hermitian matrices, i.e. non-symmetric matrices, the factorisation is on the form $A = LU$, where U is the corresponding upper triangular matrix to L. The factorisation is then used to obtain the solution vector. Two successive back substitutions are then performed; first $Ly = b$ in the symmetric case and $Uy = b$ for non-symmetric matrices, then $Lx = y$. The computation of the back substitutions require less

arithmetic computations compared to computing L and U, hence the computation of the factorisation is the most expensive part.

When using a direct solver, ill-conditioned matrices are solvable and the factorised matrix can be reused and applied for solutions of several right hand sides. These solvers can be used without a lot of adjustments done by the user, and as they are based on algebra and graph theory and not on any specific construction of the system of equations, they are versatile and independent of application.

However, there are some drawbacks using direct solvers. The need of building the entire matrix of the system is often present, hence they may not be usable for large systems as the storage of the matrix demands too much memory. Other memory requirements are also present. As the number of equations and grid size increases, memory requirements for storage of numerical factor and operation count grow rapidly, especially for 3D computations. Another disadvantage is that direct solvers do not benefit on the distinctive qualities of the problem due to their abstract/universal approach. They are also harder to make parallel on a large number of processors in an efficient way, and for non-incremental methods, that is for methods where the matrix A has to be computed for each iteration, the solution must be completely recomputed.

A direct solver will be used in WAFLE as the code will be integrated to another already existing code (FANTOM) which is based on direct solvers. The direct solver PARDISO is the one used, and this solver makes extensive use of basic scalar and parallel algebraic functions libraries (BLAS and ScaLAPACK). Hence, their efficiency is mostly affected by the quality of the implementation of these low level routines on the computer used for the computations.

5.4.1 BLAS and LAPACK

Basic Linear Algebra Subprograms (BLAS) was first published in 1979 in order to, among other reasons, reduce the amount of executed time in low level operations. BLAS is a application programming interface standard for performing basic operations of numerical linear algebra such as vector and matrix multiplications. They are used to build larger packages as LAPACK and are heavily used in high-performance computing.

Linear Algebra PACKage (LAPACK) is a software providing routines for solving system of linear equations and linear least-squares, eigenvalue problems and singular value problems. LAPACK is written in FORTRAN 90 and the associated matrix factorisation, such as LU, Cholesky, QR and Schur, are also provided. The software are able to handle dense and banded matrices, but not sparse matrices in general. The routines treats both real and complex matrices in both single and double precision.

5.4.2 PARDISO

PARDISO (Parallel Sparse Direct Solver) [17, 18] is a software package for solving large sparse symmetric and nonsymmetric linear systems of equations on shared

memory multiprocessors. The software is high-performance, robust and memory-efficient and easy to use. PARDISO was first released in 2004 and since its release, the software has been licensed to thousands of researchers at international scientific laboratories and universities.

The software package calculates the solution of a set of sparse linear equations with multiple right hand sides, $AX = B$, using a parallel LU, LDL or LL^T factorisation, where A and X are n by n matrices and B is a n by $nrhs$ matrix. The figure below shows the features of the PARDISO package: Unsymmetric, structurally symmetric or symmetric systems, real or complex, positive definite or indefinite, Hermitian are all solvable by PARDISO. Within the software, an automatic combination of iterative and direct solver algorithms is built to accelerate the solution process for very large 3-dimensional systems.

5.5 Benchmarking

The word benchmark refers to a set of programs or program segments that are used to measure performance. When developing a computer program, various benchmarks are used to verify and validate the results produced by the program. This consists in evaluating the software to determine whether the products of a given development phase satisfy the conditions imposed at the start of that phase (verification) and evaluating the software during or at the end of the development process to determine whether it satisfies specified requirements (validation).

Benchmarking can be done by comparing the numerical solutions obtained by solving the system of linear equations with

1. analytical solutions,
2. results of physical (analogue) experiments,
3. numerical results from other (well-established) codes,
4. general physical considerations.

Benchmarking of newly created tools is absolutely necessary, although often very tedious, as this is the only way to gain some confidence that the numerical modelling tool correctly reproduces a number of challenging models. When benchmarking WAFLE, mostly the numerical results obtained have been compared to analytical solutions, but also results from other codes have been used [11].While performing these benchmarks on WAFLE, we use bilinear polynomial on bilinear quadrilateral elements.

5.6 Selected types of benchmarks

The benchmarks described in this chapter look at the similarity between the results obtained by WAFLE and the corresponding analytical results or results obtained by other well-tested numerical programs [11].

5.6.1 Diffusion benchmark

The first two benchmarks are concern with the diffusion equation or heat equation in one and two space dimensions respectively. The equation of interest arises from the general form of our model equations for energy (4.20), when setting the advection term, $\mathbf{v} \cdot \nabla u$, to zero, as well as the term for the generative forces, σu, and the term for sinks and source, q:

$$\frac{\partial u}{\partial t} - \nabla \cdot (\kappa \nabla u) = 0, \tag{5.10}$$

where u is the unknown quantity. Assuming κ is independent of space within the given domain Ω, setting $\kappa = 1$ for simplicity, and stating initial and boundary conditions, the problem can be stated as

$$\begin{aligned} \frac{\partial u}{\partial t} - \Delta u &= 0 \qquad \text{in } \Omega, \\ u &= 0 \qquad \text{on } \partial\Omega \times [0, \infty), \\ u &= g \qquad \text{on } \Omega \times \{t = 0\}, \end{aligned} \tag{5.11}$$

where g is a function defined such that $g : \Omega \to \mathbb{R}$.

An analytical solution to the heat equation can be found by separation of variables, as done in [5].

One-dimensional diffusion

The first benchmark tested, is a 1D benchmark of pure diffusion where κ in equation (5.10) is regarded as independent of space and time. Hence, the equation solved is

$$\frac{\partial T}{\partial t} = \kappa \Delta\, T\ , \tag{5.12}$$

where κ is the thermal diffusivity, $\kappa = \frac{k}{\rho c_p}$.

We consider a system with initial uniform temperature of 100℃ which is heated from below. The temperature at the top of the system is equal to the initial temperature of the whole system, 100℃, while the imposed temperature at the bottom is 150℃. The calculations are performed on a domain of size $[0, 1] \times [0, 1]$ consisting of 50×50 elements.

The analytical result for modelling diffusion is based on the complementary error function, erfc, and is derived by considering the fundamental solution of the heat equation (5.11) in one space dimension, see [5]. The analytical solution, in a temperature-y-coordinate system, is,

$$T_{\text{analytical}} = \text{erfc}(\frac{y}{2\sqrt{\kappa t}})(T_b - T_t) + T_t, \tag{5.13}$$

where y is the distance from the bottom to the top of the system in consideration, T_b is the temperature imposed at the bottom of the system and T_t is the temperature

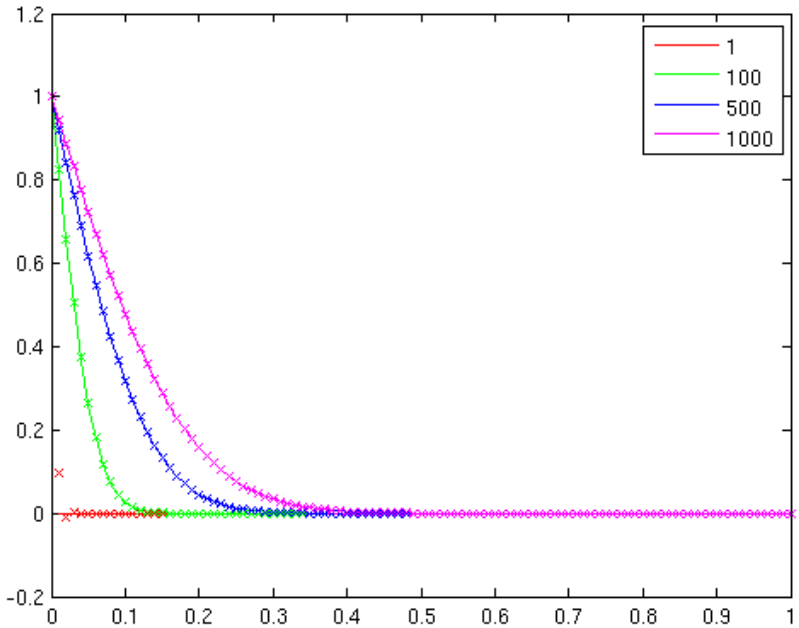

Figure 5.2: The numerical solution for the 1D diffusion benchmark is plotted against the analytical solution for the time after one, 100, 500 and 1000 timesteps. The solid line is the analytical solution, while the numerical solution obtained is marked by crosses.

imposed at the top. The solution obtained after one, 100, 500 and 1000 timesteps is shown in Figure 5.2.

Figure 5.3 shows the relative error to the solution, and we see that the solution is computed has an relative error of order $\mathcal{O}(10^{-1})$ after one timestep and decreases to $\mathcal{O}(10^{-4})$ when the solution is computed after 500 timesteps.

The error function, often called the Gauss error function, is a special function of sigmoid shape that occurs in probability, statistics, material science and partial differential equations. The error function and the complementary error function (Figure 5.4) are defined, respectively, as:

$$\begin{aligned} \mathrm{erf(x)} &= \frac{2}{\sqrt{\pi}} \int_0^x e^{-t^2} dt, \\ \mathrm{erfc(x)} = 1 - \mathrm{erf(x)} &= \frac{2}{\sqrt{\pi}} \int_x^\infty e^{-t^2}. \end{aligned} \tag{5.14}$$

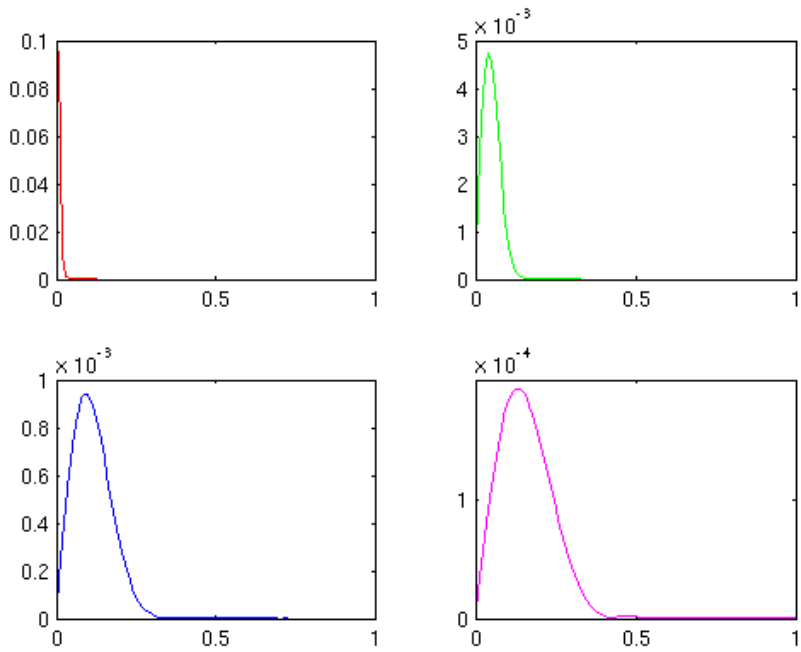

Figure 5.3: The relative error of the solution computed after one, 100, 500 and 1000 timesteps.

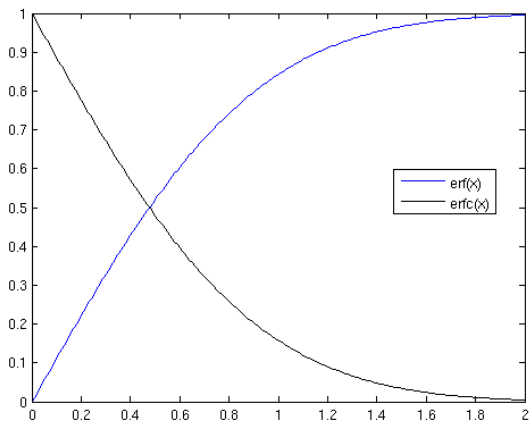

Figure 5.4: Error functions.

Second diffusion benchmark

We now consider the diffusion equation in two dimensions,

$$\frac{\partial T}{\partial t} = \kappa \Delta\, T \ , \tag{5.15}$$

where the thermal diffusivity, $\kappa = \frac{k}{\rho c_p}$, is as for the first diffusion benchmark, regarded as constant.

In this benchmark we impose a Gaussian temperature profile and let it diffuse in time, that is, placing a hot body (of max 150℃) in a cold environment(100℃). Consider the unit square $[0,1] \times [0,1]$ as our domain Ω consisting of 50×50 cells. The temperature profile is placed in the centre of the domain, and we observe how it diffuses in time. The initial temperature field is set to 100℃, and the maximum temperature of the Gaussian temperature profile is 150℃. The diffusion observed should be similar to the diffusion process described by the analytical solution given by the Gaussian function

$$T(x,y,t) = \frac{t_0}{t} \exp(-\frac{(x-x_0)^2 + (y-y_0)^2}{4\kappa t}). \tag{5.16}$$

This function describes a Gaussian pulse which gradually decreases in height and broadens in width in such a manner that its area is conserved. In equation (5.16), t_0 is the initial time and (x_0, y_0) is the initial position of the temperature pulse.

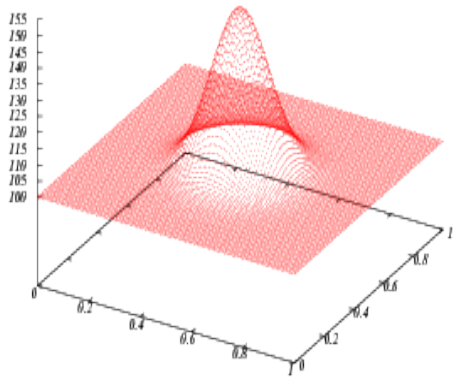

Figure 5.5: The initial state for the Gaussian hill.

Figure 5.6 shows the solutions obtained after one and 500 timesteps. Both numerical and analytical solutions are plotted. The relative error between the numerical solution computed and the analytical solution is shown in Figure 5.7. The maximum relative error for the solution computed at the first timestep is of $\mathcal{O}(10^{-3})$, while the solution after 500 timesteps has an accuracy of $\mathcal{O}(10^{-4})$.

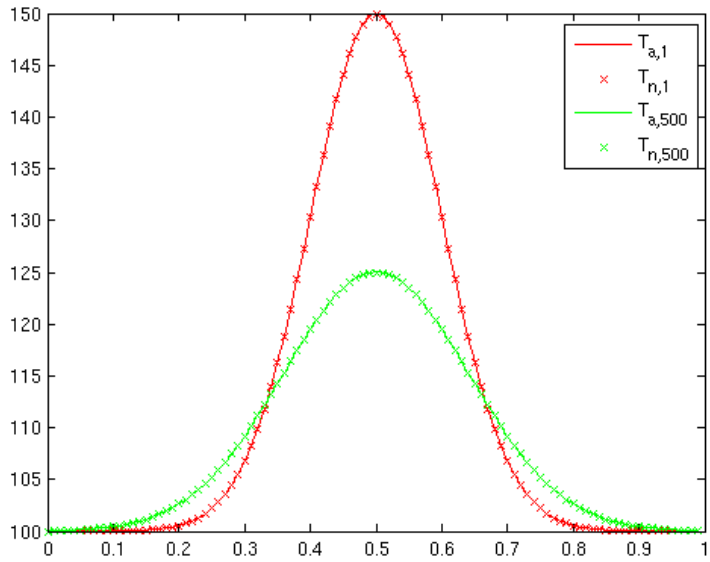

Figure 5.6: The numerical and the analytical solution after one timestep and after 500 timesteps for the Gaussian hill is computed. The numerical solutions $T_{n,1}$ and $T_{n,500}$, computed after one and 500 timesteps respectively, is marked with crosses while the solid line is the analytical solutions computed after one ($T_{a,1}$) and 500 ($T_{a,500}$) timesteps.

5.6.2 Advection benchmark

Rotating cone

This benchmark in two space dimensions is applied for characterising the limitations of the advection scheme implemented in WAFLE. The heat production term in (3.3) is set to zero, as is the diffusion term $\phi\nabla\cdot(k\nabla T)$, and we consider no heat transfer. Hence, the equation evaluated is

$$\frac{\partial T}{\partial t} + \frac{1}{\phi}\mathbf{v}\cdot\nabla T = 0, \tag{5.17}$$

where κ is constant. When deriving the analytical solution for this equation (5.17) in two space dimensions, we will use the method of characteristics and $T = T(\mathbf{x}, t) = T(x, y, t)$. The initial condition is

$$T(\mathbf{x}, 0) = T_0(\mathbf{x}) \tag{5.18}$$

Hence the initial temperature is only a function of space.

Characteristics in one space dimension, may be defined as curves $x = x(t)$ in the t-x plane and the partial differential equation (PDE) in question becomes an ordinary differential equation along these curves. Consider $\mathbf{x} = \mathbf{x}(t)$ as a characteristic curve

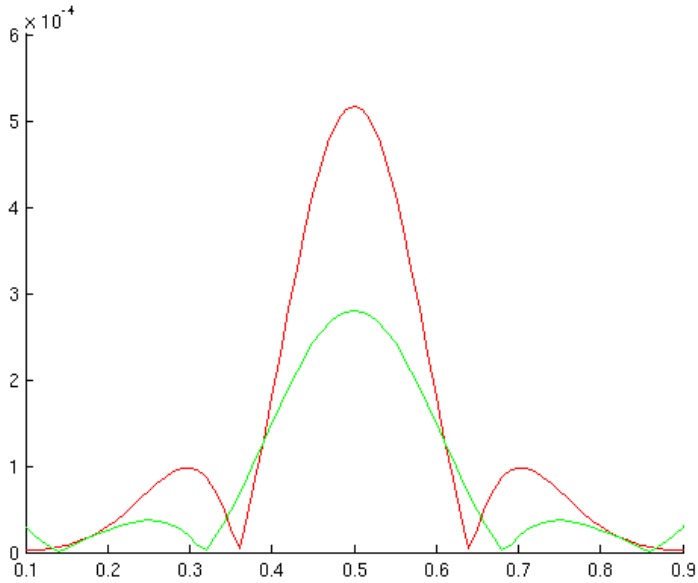

Figure 5.7: Graf over the relative error for the solution of the Gaussian hill computed after one and 500 timesteps. The red line drawn, is the relative error obtained for one timestep. The relative error after 500 timesteps is shown in green colour.

in two space dimensions, and regard T as a function of time, $T = T(\mathbf{x}(t), t)$. The rate of change of temperature along $\mathbf{x} = \mathbf{x}(t)$ is

$$\frac{dT}{dt} = \frac{\partial T}{\partial t} + \frac{d\mathbf{x}}{dt}\frac{\partial T}{\partial \mathbf{x}}, \tag{5.19}$$

if the characteristic satisfies the ODE problem

$$\frac{d\mathbf{x}}{dt} = \mathbf{v}, \tag{5.20}$$

where the speed $\mathbf{v}$ is called the characteristic speed, then the PDE in (5.17) together with (5.19) and (5.20) gives

$$\frac{dT}{dt} = \frac{\partial T}{\partial t} + \mathbf{v}\frac{\partial T}{\partial \mathbf{x}} = 0. \tag{5.21}$$

From this, the rate of T along the characteristic curve $\mathbf{x} = \mathbf{x}(t)$ is zero, thus T is constant along $\mathbf{x} = \mathbf{x}(t)$. For a problem in one space dimension, let a be the characteristic speed. According to (5.20), the speed a is the slope of the curve $x = x(t)$ in the t-x plane. Sketching the curve in an x-t plane, the slope is $\frac{1}{a}$ for the curves drawn.

In two space dimensions, suppose $\mathbf{x}(0) = \mathbf{x}_0$. Then the characteristics through

the initial point $(\mathbf{x}_0, t) = (x_0, y_0, t)$ is $\mathbf{x} = \mathbf{x}_0 + \mathbf{v}t$. Hence the initial condition $T(\mathbf{x}, 0) = T_0(\mathbf{x})$ at $t = 0$ give the solution

$$T(\mathbf{x}, t) = T_0(\mathbf{x}_0) = T_0(\mathbf{x} - \mathbf{v}t), \tag{5.22}$$

for the characteristic passing through the initial point $\mathbf{x}_0 = (x_0, y_0)$ in the x-y plane.

In this benchmark, we will consider a full 2π-rotation for a temperature field described by a cosine-function. According to the analytical solution obtained above, when the cone is rotated a full 2π-rotation, the cone should retain its shape and size, i.e. the height and width of the cone should be preserved and the temperature field should be equal to its initial state.

The set up for this benchmark is similar to the one used by Donea and Huerta in [11]. The initial temperature field is defined as

$$T(x, y) = \begin{cases} \frac{1}{4}(1 + \cos \pi X_1)(1 + \cos \pi X_2) & \text{if } X_1^2 + X_2^2 \leq 1, \\ 0 & \text{otherwise,} \end{cases}$$

where $\mathbf{X} = \frac{\mathbf{x} - \mathbf{x}_0}{\sigma}$, and the temperature field is set to zero on the boundary. The maximum initial temperature of the cone is 1℃. The initial position of the centre is $\mathbf{x}_0$, and the radius of the cosine hill is σ. As in [11], we placed the initial position in the uppermost right part of our domain and let the radius of the cone be $\sigma = 0.2$. Our domain is the unit square $[0, 1] \times [0, 1]$, hence $\mathbf{x}_0 = (\frac{2}{3}, \frac{2}{3})$, see Figure 5.10. We have employed a uniform grid, 30×30 quadrilateral elements, over our domain in the calculations. The velocity field is a pure rotation field with unit angular velocity, $\mathbf{v}(\mathbf{x}) = (-x_2, x_1)$.

Figure 5.9 shows the contours for the initial temperature field and for the temperature field after a full 2π-rotation. Comparing these results to the ones obtained by Donea and Huerta in [11] for the Crank-Nicholson/Galerkin method, which will be equivalent to using the trapezoidal/Galerkin method for other elements than triangles, a certain similarity is visible. Donea and Huerta performed the experiment with a timestep $\Delta t = 2\pi/120$, while the result shown in Figure 5.9 is obtained with a timestep $\Delta t = 2\pi/200$. Without having the exact information about the complete set up used by Donea and Huerta, it is difficult trying to simulate their experiment.

Propagation of a steep front

This is a benchmark in one space dimension where convection at unit speed of discontinuous initial data is considered. The benchmark is yet another test for the advection scheme and quite a challenging one as discontinuities often lead to large oscillations and instability may occur. The discontinuity occurs over one element and is initially located at $x = \frac{L_x}{4}$ of the computational domain $[0, 1]$. The trapezoidal rule is applied for the time-discretisation in this benchmark.

As for the previous benchmark, the rotating cone, the equation evaluated is

$$\frac{\partial T}{\partial t} + \frac{1}{\phi}\mathbf{v} \cdot \nabla T = 0, \tag{5.23}$$

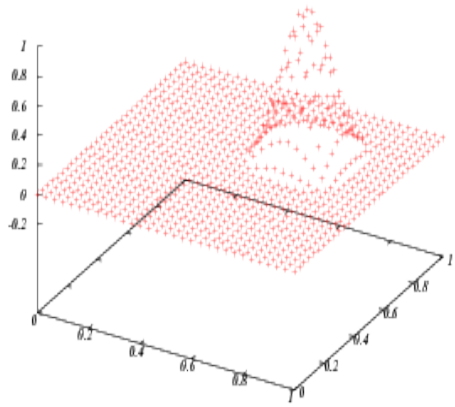

Figure 5.8: The initial state for the cosine hill.

where the initial inlet condition $T(0,t) = 1$ is imposed. The initial temperature at the discontinuity, $T(x = L_x/4, 0)$ is set to zero. A uniform grid of bilinear quadrilateral elements, 50×50, is employed. We have advected the front from its initial position $x = \frac{L_x}{4}$ to its final position $x = \frac{3L_x}{4}$ at $t = t_{end}$. The test has been carried out with the Courant number $C = 0.5$.

The case we want to recover, is shown in Figure 5.11.

Solving this problem using a pure Galerkin scheme where the time discretisation is done by applying the trapezoidal rule, is not desirable due to the oscillations obtained as shown in Figure 5.12.

From the previous chapter, Section 4.3, this behaviour of the solution is expected due to the nonsymmetry that arises from the advection term. To attain a better approximation to the analytical solution, we have performed a naive approach in order to reduce the error. This approach is based upon the paper of Braun [14], where a streamline-upwind Petrov-Galerkin method is used to improve stability:

$$N^* = N + \tau \mathbf{v} \cdot B, \tag{5.24}$$

where N is the shape functions, B is the derivative of the shape functions in space, $\mathbf{v}$ is the velocity and τ is a factor applied to improve stability.

A reasonable choice for τ is to define it in terms of the mesh parameter h and the velocity $\mathbf{v}$ [11]. We set

$$\tau = \gamma \frac{h}{||\mathbf{v}||}, \tag{5.25}$$

and search for a value for γ that will reduce the error obtained for the propagation

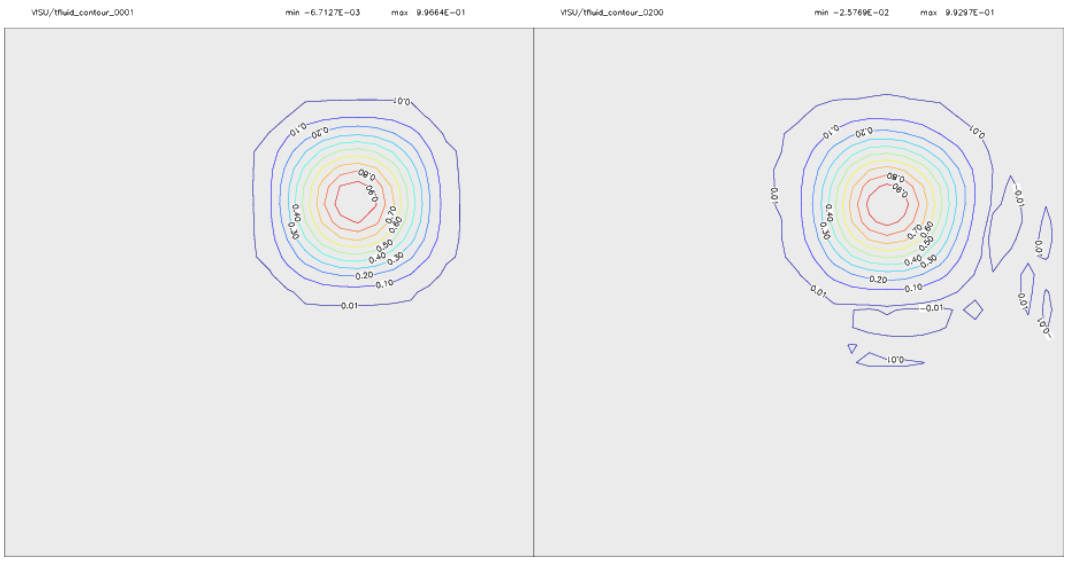

(a) Initial state. (b) After a 2π-rotation.

Figure 5.9: Contour plots of the temperature field.

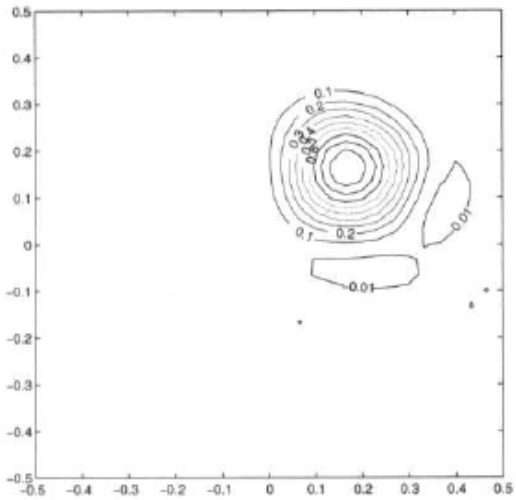

Figure 5.10: Numerical solution obtained by Donea and Huerta after a complete revolution using the Crank-Nicholson/Galerkin method. $\Delta t = 2\pi/120$.

of a steep front. We let γ vary between 0 and 0.1 and observe the impact different values of γ have on the numerical solution. Figure 5.13 shows the effect of the γ-parameter for $\gamma = 0.002, 0.020, 0.040$. For $\gamma = 0.1$, we obtain an over-diffusive scheme, see Figure 5.14. Then the question is, which value of γ should be chosen in order to achieve a more stable, but not over-diffusive scheme. The answer depends

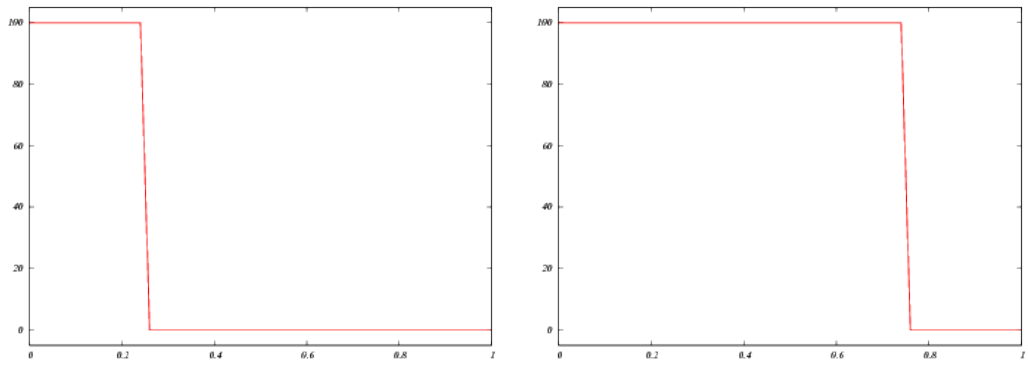

(a) Initial state (b) At time $t = t_{end}$

Figure 5.11: Propagation of a steep front: Analytical solution.

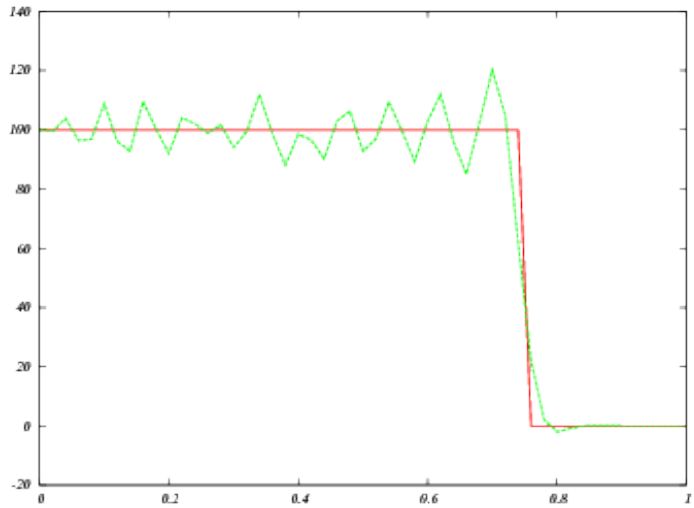

Figure 5.12: Propagation of a steep front: Pure Galerkin.

upon the problemat hand, but for general cases, a value around $\gamma = 0.045$ gives an error of less than 0.1% and the diffusion will not be to large. This is shown in Figure 5.15.

The approach presented by Tezduyar and Osawa in [15], as introduced in Chapter 4, has a τ_{SUPG}-parameter given by

$$\tau_{SUPG} = \left(\frac{1}{\tau_1^r} + \frac{1}{\tau_2^r} + \frac{1}{\tau_3^r}\right)^{-\frac{1}{r}}, \tag{5.26}$$

with

$$\tau_1 = \frac{h}{2v}, \tag{5.27}$$

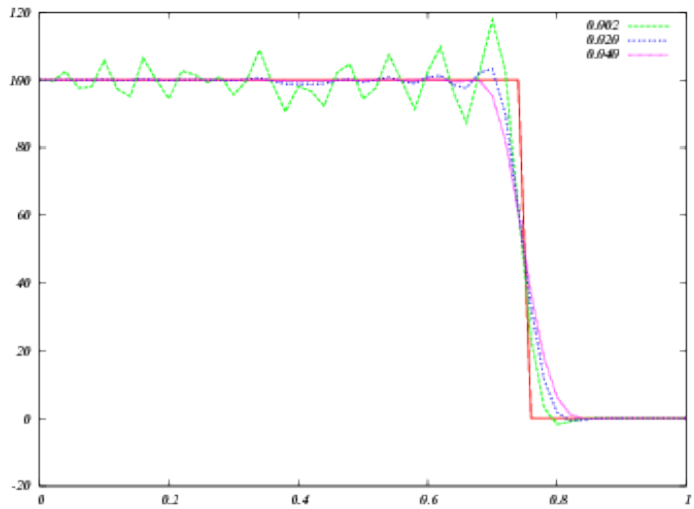

Figure 5.13: Propagation of a steep front: $\gamma = 0.002, 0.020, 0.040$.

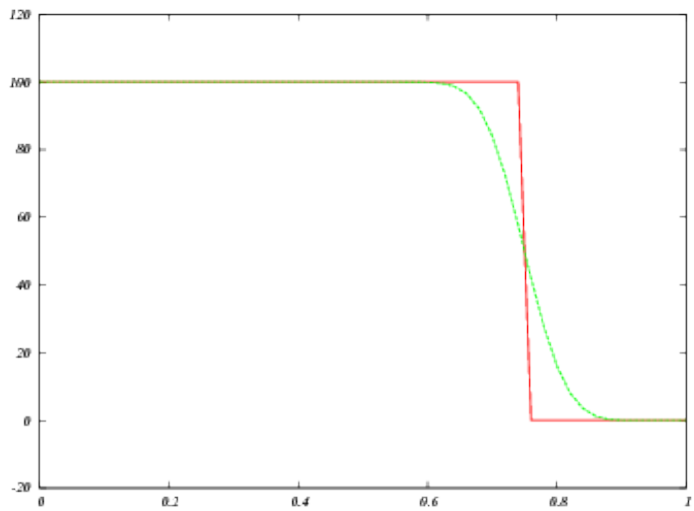

Figure 5.14: Propagation of a steep front: $\gamma = 0.1$.

$$\tau_2 = \theta \Delta t, \tag{5.28}$$

$$\tau_3 = \frac{h^2}{4\alpha} = \frac{h^2 \rho c_p}{k}. \tag{5.29}$$

The parameters τ_1, τ_2 ad τ_3 are, as presented earlier in Chapter 4, the popular limits for the advection-dominated, the transient-dominated and the diffusion-dominated cases respectively. We use $r = 1$ for simplicity.

As described in Chapter 4, the parameter for the transient-dominated case τ_2,

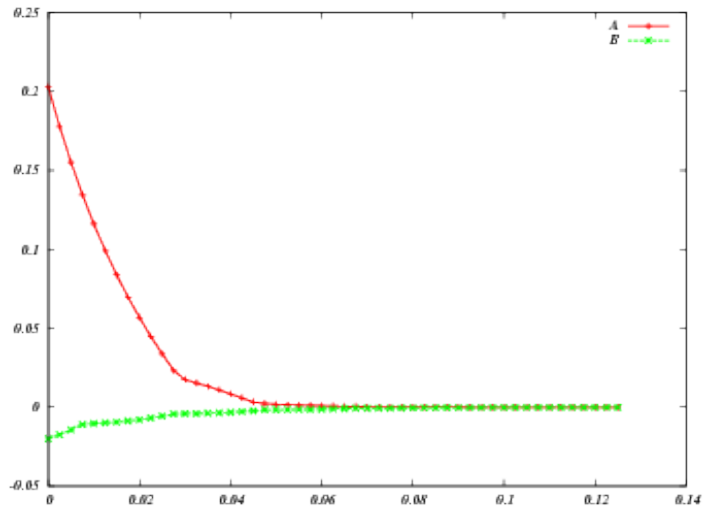

Figure 5.15: Plot over the relative error obtained for different values of γ, where A is the maximum relative error measured at the top of the front while B is the maximum relative error measured at the bottom of the front.

can be expressed as follows for this benchmark:

$$\tau_2 = \theta C \frac{h}{||\mathbf{v}||}. \tag{5.30}$$

As the heat conductivity is zero, $\tau_3 = \infty$, and hence, τ can be expressed as

$$\tau_{SUPG} = \frac{h}{||\mathbf{v}||}\left(2 + \frac{1}{\theta C}\right)^{-1}, \tag{5.31}$$

where θ is the parameter for the θ-family methods, C is the Courant number, h is the mesh size and $\mathbf{v}$ is the velocity. In our case, $\theta = 1/2$ and $C = 1/10$. Hence,

$$\tau_{SUPG} = \frac{h}{||\mathbf{v}||}\frac{1}{22}. \tag{5.32}$$

When this is related to our first approach, we see that choosing $\gamma = 1/22$ would correspond to this estimate for τ_{SUPG}. From Figure 5.15, $\gamma = 0.045$ seems to be a reasonable value. This is pretty close to the estimate obtained by the approach of Tezduyar and Osawa as

$$\gamma = \frac{1}{22} \cong 0.045. \tag{5.33}$$

5.6.3 Heat production

This is a benchmark for testing the heat production term only. We will then consider the model equation without advection, conduction and heat transfer. The model

equation is then reduced to

$$\frac{\partial T}{\partial t} = \frac{H}{c_P}, \tag{5.34}$$

where H is the heat production. We will consider a system with a uniform temperature field that is heated due to internal heat production. In order to prevent oscillations in the numerical solution, the boundary conditions imposed are based on the analytical solution

$$T(t) = \frac{H}{c_P} t + T_0, \tag{5.35}$$

with $T_0 = 100$ ℃. When the boundary conditions are set to a constant value, e.g. $T_b = 100$, then oscillations occur due to the discontinuity in the temperature field between the temperature at the boundary and the temperature inside the domain as the temperature inside the domain increases in time. The temperature inside the domain follows the analytical solution up to a certain order, $\mathcal{O}(10^{-7})$.

5.7 General comments about WAFLE

WAFLE is a portable code, as the only thing needed is a fortran compiler since the solver used, PARDISO, is free. As already mentioned in section about the set up of WAFLE, the porosity is a field which can vary in space. Another feature of the numerical tool is that the permeability $\mathbf{K}$ is a tensor, which allows for anisotropic cases. It is then possible to apply the code for other areas of interest than just modelling convection in geothermal systems. For instance can WAFLE be a possible application to CO_2-storage [19].

Two coupled model equations for energy are implemented in WAFLE, one for the fluid and one for the solid. Thus, systems where the temperature of the solid differ from the temperature of the fluid can be solved. The implementation and setup of the different materials (solid and fluid) are created such that an extension to systems consisting of more than two materials can be made. This could be interesting, for instance, in the case of layered lithologies.

For the pressure field, both Neumann and Dirichlet boundary conditions are implemented. The Neumann boundary conditions allow for presence of injection wells. Hence, with some modifications, systems with injection and production wells can be solved which would be of interest in cases where exploitation of the heat in geothermal systems is requested. Periodic boundary conditions are also implemented and can be toggled on/off.

A final remark; a debug mode is implemented in WAFLE for debugging purposes with additional outputs.

Chapter 6

Preliminary numerical results

The numerical tool created demands a lot more of testing and benchmarking to achieve confidence in the results obtained when running, and to explore the limits and advantages of the code. The development of the code has just completed the first level in the process of establishing a proper numerical modelling tool. Hence, not a lot of numerical results have been achieved yet, but in this chapter we will present some preliminary results obtained for steady state convection in porous media.

6.1 Measure and computation of Rayleigh numbers and corresponding Nusselt numbers

The Rayleigh-Darcy number is defined in Chapter 3 as

$$RaDa = \frac{\rho^2 c_p g \beta \ \Delta T \ LK}{\mu k}, \tag{6.1}$$

where ρ is the density, c_p is the heat capacity, g is the gravity, β is the thermal expansion coefficient, T is the temperature, L is the length scale, K is ther permeability, μ is the dynamic viscosity and k is the heat conductivity. During the numerical computations performed in this chapter, the heat conductivity is the only value varied in order to change the Rayleigh number. All other material properties are kept constant.

6.1.1 The critical Rayleigh-Darcy number

A brief introduction to linear stability analysis was given in Chapter 3. The onset of convection in porous media is given by the critical Rayleigh-Darcy number, $RaDa_c$, and linear stability analysis gives that $RaDa_c = 4\pi^2$ for porous media.

For a Rayleigh-Darcy number lower than the critical value, no convection occurs and the heat transfer is only due to diffusion. At this stage, the system is stable,

and the heat flux is given by

$$q_d = -k\nabla T = -\frac{k\Delta T}{L_y}, \tag{6.2}$$

where k is the heat conductivity, T is the temperature of the fluid and L_y is the vertical length scale.

When the $RaDa$ number exceeds the critical value $RaDa_c$, convection cells occur and the heat is now transported by both advection and diffusion processes. In addition to the critical number for the onset of convection, there exist other critical values for the Rayleigh-Darcy that increases the number of convection cells when $RaDa$ exceeds these values.

The critical Rayleigh-Darcy number proves to be difficult to determine. Test runs on WAFLE, shows that the Rayleigh-Darcy number seems to be dependent of the grid resolution, and as closer $RaDa$ is to $RaDa_c$, longer time is needed in order to reach steady state. Hence, very long runs have to be performed for Rayleigh-Darcy close to the critical value. However, the preliminary results so far, indicate a value of $RaDa_c \approx 50$, a value that is higher than the expected theoretical critical Rayleigh-Darcy number and further investigation is needed in order to explain the deviation.

6.1.2 Computation of Rayleigh-Darcy numbers and corresponding Nusselt numbers

The Nusselt number is defined as the ratio of convective to conductive heat transfer across a boundary, that is, the ratio of the heat transferred due to advection to the heat transferred due to diffusion. This can be expressed in terms of the diffusive heat flux q_d and the total heat flux q_T of the system. The total heat flux can be measured at the top of the domain and averaged over the whole length. The Nusselt number can then be found by

$$Nu = \frac{\textit{Total heat flux}}{\textit{Diffusive heat flux}} = \frac{k\nabla T}{k\Delta T/L_y}. \tag{6.3}$$

From this expression, the Nusselt number is obviously equal to unity for $RaDa$ lower than the critical value.

In the setup for the system for computation of $RaDa$ and Nu, we are considering a system that is heated from below. We have employed a grid consisting of 120×30 elements and horizontal periodic boundary conditions are imposed, except for the last case where $RaDa = 274.7$. Then the grid consists of 200×50 elements. The temperature at the top T_t, is set to 100℃, while the temperature at the bottom of the domain is higher, $T_b = 110$℃. The initial temperature field in the system is defined as a linear gradient between T_b and T_t with a randomness of 1% to trigger the instabilities needed for convection to occur. Figure 6.1 shows the physical domain with initial conditions.

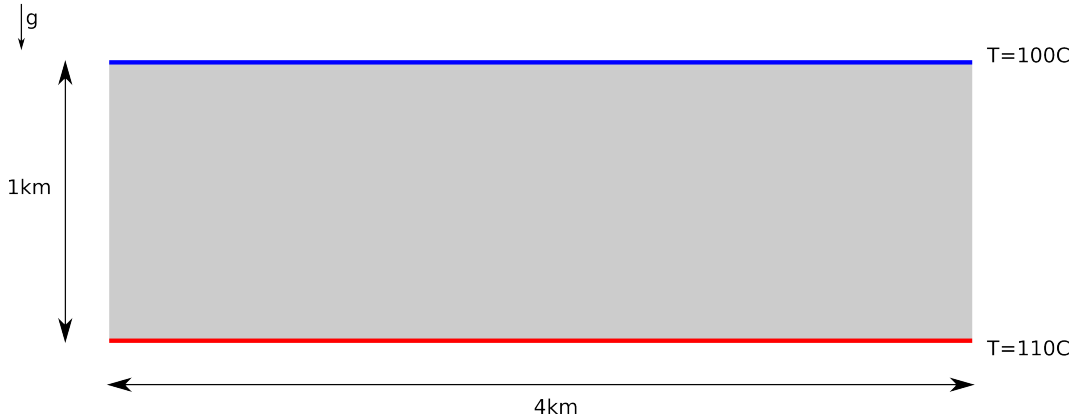

Figure 6.1: The domain of interest for computations of $RaDa$ and Nu

At the beginning of the simulation, Nu is indeed equal to unity with an error of 0.05%. When convection starts, Nu increases progressively and finally stabilises when steady state is reached. This behaviour is similar to the behaviour of the velocity, see Figure 6.2. The convection cells obtained for $RaDa = 63.4$, $RaDa =$

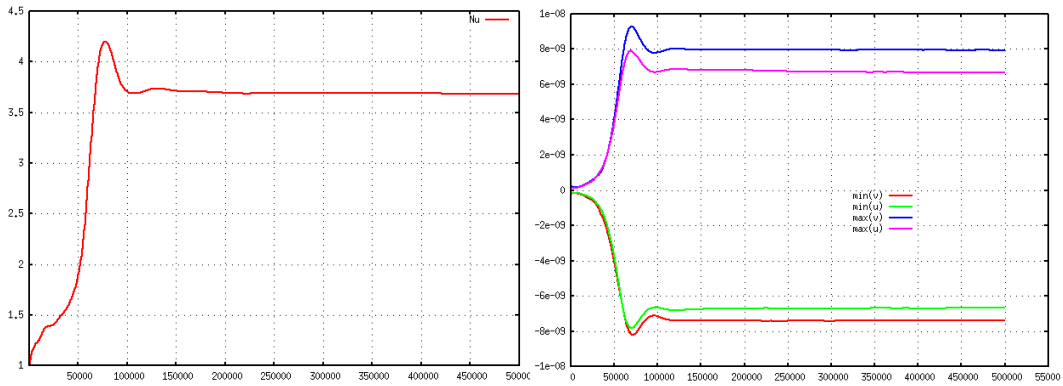

(a) Nusselt number

(b) Velocity: The red line is min(v), the green is min(u), the blue is max(v) and the purple is max(u), where v and u denotes the vertical and horizontal components of the velocity respectively.

Figure 6.2: Behaviour of the Nusselt number and the velocity towards steady state.

108.4 and $RaDa = 274.7$ is shown in Figure 6.3,6.4,6.5 respectively.

The scaling of the relationship between the Rayleigh-Darcy number and the Nusselt number was published in 1972 by Palm et al. [20], and we are comparing our results to them in Figure 6.6. The blue points are the values obtained by WAFLE. The red point are obtained with another FEM-code, created as part of

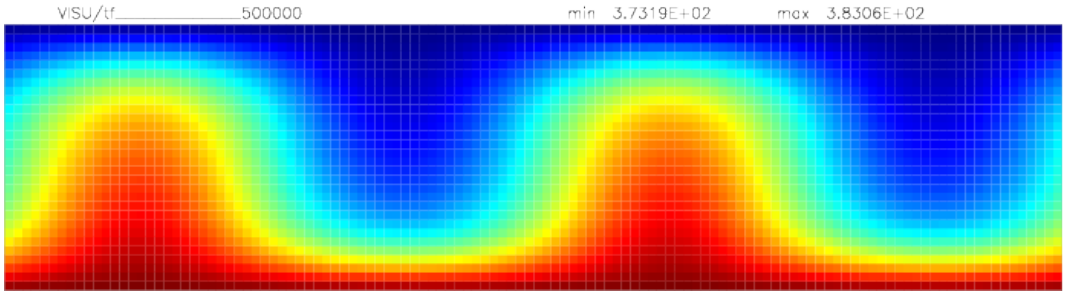

Figure 6.3: Convection cells for $RaDa = 63.4$

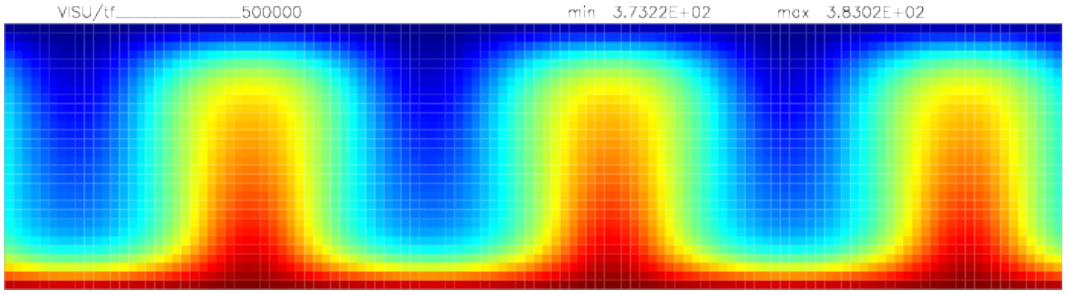

Figure 6.4: Convection cells for $RaDa = 108.4$

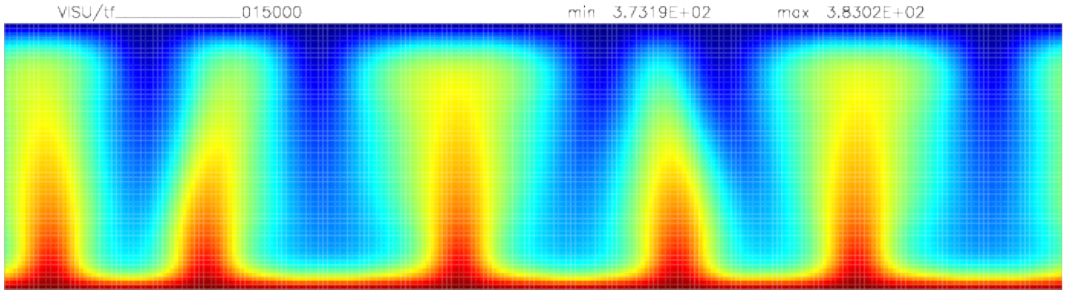

Figure 6.5: Convection cells for $RaDa = 274.7$

a project at Physics of Geologic Processes, University of Oslo by A. Souche [1] and M. Dabrowski [2]. Their numerical program is using higher order (Q_2) elements, and their results seem to follow the experimental trend to a larger extent than WAFLE. An adequate comparison of the results of the two modelling tools is not possible as the grid used for the computations with WAFLE is a lot coarser than the grid used by A. Souche and M. Dabrowski.

One of the computations for the Nusselt number using WAFLE, seems to fit

[1] Alban Souche, ph.D. student, Physics of Geological Processes, University of Oslo, Norway. Private communication

[2] Marcin Dabrowski, Post doktor, Physics of Geological Processes, University of Oslo, Norway

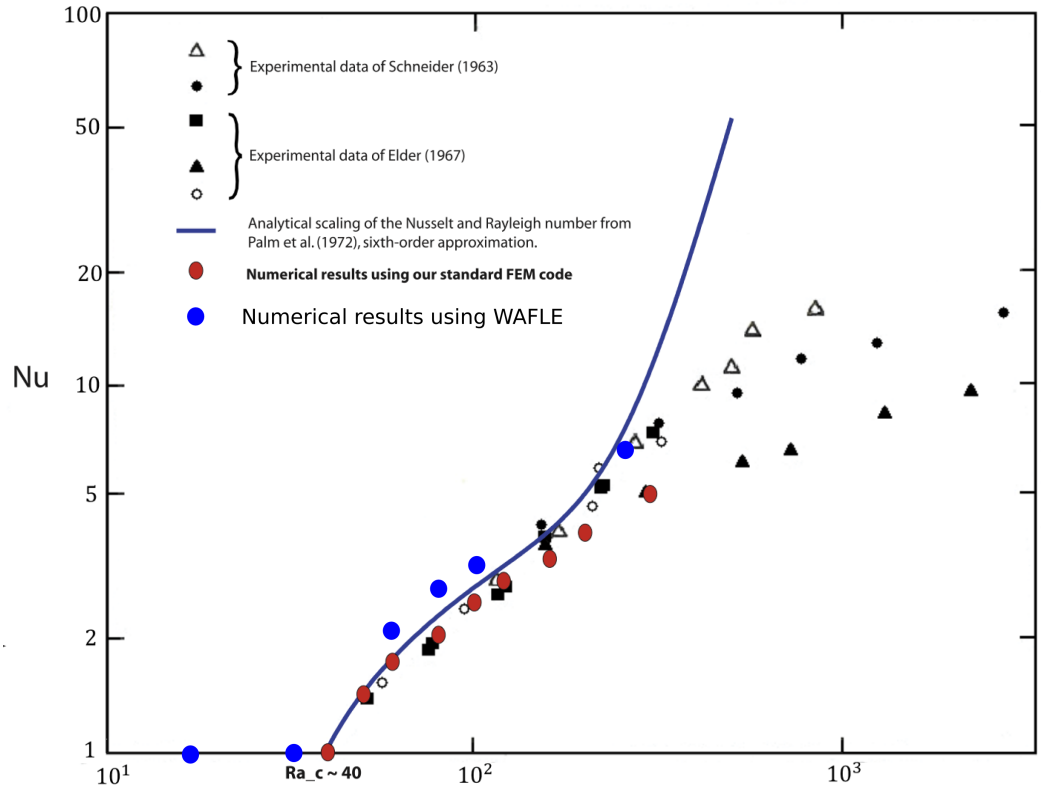

Figure 6.6: Relationship between $RaDa$ and Nu. The red points are the results obtained by A. Souche and M. Dabrowski, while the blue points are obtained using WAFLE.

better to the curve by Palm et al. in [20] than the others. This is the rightmost blue point, computed for $Ra = 274.7$. This simulation is done with a rather refined grid, and may be an indication of a grid dependency in the computation of the Rayleigh-Darcy number. However, at this stage, further investigation is needed before any conclusion can be drawn.

Chapter 7

Summary and further work

In this thesis, a new numerical modelling tool, WAFLE, based on the finite element method is presented. WAFLE stands for WAter FLow Equation solver which solves mass, momentum and heat transfer equations in two dimensions in porous media. The program still requires a lot of research and benchmarking to fully understand its behaviour, limitations and advantages.

The implementation of the WAFLE is naive in the sense that only linear quadrilateral elements with bilinear polynomials are used. However, the results from the tests and benchmarks performed so far, indicates that the code are able to reproduce results obtained by more well-tested programs [11].

7.1 Summary

Several of WAFLE's features have not yet been tested and/or explored, and will demand a lot of benchmarking. Some of the benchmarks already performed, show that the modelling tool is able to produce satisfactory results, while others expose limitations. One of them, the propagation of a steep front, enlightened the issue of the treatment of the advection term with standard finite elements. This benchmark shows that when using a simple approach with standard Galerkin method for the advection term, instability and large oscillations occur. Another approach was then attempted; the SUPG-method. When the SUPG-method was applied for the specific problem at hand, results of higher accuracy were obtained.

Still, further investigation of different methods for dealing with the advection term is needed to gain more knowledge about how this term should be treated to avoid the instabilities arisen when solved by finite elements.

In Chapter 6, some preliminary results for computation of the Rayleigh-Darcy number and the Nusselt number were shown. As the numbers obtained deviate from the expected theoretical value, further investigation is needed. The indication that the computation of the Nusselt number depends on the grid size, should be studied.

Features

The most important features of WAFLE is listed below:

1. Portable code.
2. Two energy equations, one for solid and one for fluid: can solve for systems where the temperature of the solid differs from the fluid temperature.
3. Porosity is a field which can vary in space.
4. The permeability is a tensor, which allows for the case of anisotropic materials.
5. Neumann boundary conditions in the heat transport case allow for presence of injection and production wells.
6. Periodic boundary conditions can be toggled on/off.
7. Built-in graphics and ASCII-output.
8. Possibility to include more than two materials.

Recommendations

A brief summary of proposed recommendations for further work is listed below:

1. Investigation of the implementation of the advection term.
2. Carrying on the studies of the critical Rayleigh-Darcy number and computation of the Nusselt number.
3. Testing the coupling between the solid and fluid when the materials have different temperatures.
4. Modelling real case scenarios/ reproducing data from geothermal systems.
5. Including wells for modelling extraction of heat.
6. Benchmarking and extensively testing of the program.

A final comment

The code needs in general a lot more testing and several benchmarks must be applied in order to detect other limitations and extend the application area of the numerical program. When WAFLE is thoroughly tested, additional extensions can be made. It is possible to allow for more than two materials, solid and fluid, which would be of interest in the case of layered lithology.

Although WAFLE is not tested as profound as one may had hoped for, it is a promising tool based on the results obtained so far and the range of possible extensions and areas of applications.

Bibliography

[1] C. Thieulot. FANTOM. http://thieulot.geo-phy.net/.

[2] J. Bear. *Dynamics of Fluids in Porous Media.* Dover Publications, Inc., 1988. ISBN 0-486-65675-6.

[3] D.A. Nield and A. Bejan. *Convection in Porous Media.* Springer, 2006. ISBN 0-387-29096-6.

[4] J.D. Murray. *Mathematical biology, 1, An introduction.* Springer, 2002. ISBN 0-387-95223-3.

[5] L.C. Evans. *Partial Differential Equations.* American Mathematical Society, 1998. ISBN 0-8218-0772-2.

[6] Z. Chen, G. Huan, and Y. Ma. *Computational Methods for Multiphase Flows in Porous Media.* SIAM, 2006. ISBN 0-89871-606-3.

[7] D. Braess. *Finite elements: Theory, fast solvers, and applications in solid mechanics.* Cambridge University Press, 2007. ISBN 978-0-521-70518-9 paperback.

[8] C. Johnson. *Numerical colution of partial differential equations by the finite element method.* Cambridge University Press, 1987. ISBN 0-521-347580.

[9] T.J.R. Hughes. *The Finite Element Method: Linear Static and Dynamic Finite Element Analysis.* Dover Publications, Inc, 2000. ISBN 0-486-41181-8.

[10] A.H. Stroud and D. Secrest. *Gaussian Quadrature Formulas.* Englewood Cliffs : Prentice-Hall, 1966.

[11] J. Donea and A. Huerta. *Finite Element Methods for Flow Problems.* John Wiley and Sons, 1988. ISBN 0-471-49666-9.

[12] R.J. LeVeque. *Finite Difference Methods for Ordinary and Partial Differential Equations: Steady-State and Time-Dependent Problems.* SIAM, 2007. ISBN 987-0-898716-29-0.

[13] R. Courant, K. Friedrich, and H. Lewy. Über die Partiellen Differentzenleichungen der Mathematischen Physik. *Mathematischen Annalen*, 1928.

[14] J. Braun. Pecube: A new finite-element code to solve the 3D heat transport equation including the effects of a time-varying, finite amplitude surface topography. *Computers & Geosciences*, 29(6):787–794, 2003.

[15] T.E. Tezduyar and Y. Osawa. Finite element stabilization parameters computed from element matrices and vectors. *Computer Metods in Applied Mechanics and Engineering*, 2000.

[16] P.B. Bohev and C.R. Dohrmann. A computational study of stabilized, low-order C^0 finite element approximations of Darcy equations. *Computational Mechanics*, 2006.

[17] 0. Schenk and K. Gärtner. Solving unsymmetric sparse systems of linear equations with PARDISO. *Journal of Future Generation Computer Systems*, 20(3):475–487, 2004.

[18] 0. Schenk and K. Gärtner. On fast factorization pivoting methods for symmetric indefinite systems. *Elec. Trans. Numer. Anal*, 23:158–179, 2006.

[19] S. Rapaka, R.J. Pawar, P.H. Stauffer, D. Zhang, and Chen S. Onset of convection over a transient base-state in anisotropic and layered porous media. *Journal of Fluid Mechanics*, 2009.

[20] E. Palm, J.E. Weber, and O. Kvernvold. On steady convection in a porous media. *Journal of Fluid Mechanics*, 1972.